

Figure 4. Abrogated Self-Renewal Capacity and Defective Maintenance of Quiescence in p27^{-/-}p57^{KD} LSK Cells

(A) The experimental scheme for shRNA transduction.

(B) Decreased colony formation of p27^{-/-}p57^{KD} LSK cells after long-term culture. p27^{+/+}p57^{CON}, p27^{+/+}p57^{KD}, p27^{-/-}p57^{CON}, or p27^{-/-}p57^{KD} GFP⁺ LSK cells (2×10^3) were cultured on OP9 stromal cells for the indicated number of weeks (W) and tested for colony formation. Data shown are the mean number (\pm SD) of colonies formed (* $p < 0.01$, $n = 3$).

(C) Hematopoietic reconstitution capacity of p27^{+/+}p57^{CON}, p27^{+/+}p57^{KD}, p27^{-/-}p57^{CON}, and p27^{-/-}p57^{KD} LSK cells. Irradiated recipient mice were transplanted with 5×10^3 GFP⁺ LSK cells and 2×10^5 competitor cells. Data shown are the mean percentages (\pm SD) of donor GFP⁺ cells in the PB at the indicated time-points post-BMT (* $p < 0.01$, ** $p < 0.05$, $n = 5$).

the engraftment defect of $p27^{-/-}p57^{KD}$ LSK cells cannot be attributed to a defect in homing or cell survival.

It was next investigated whether the repopulating defect observed with $p27^{-/-}p57^{KD}$ LSK cells could result from changes in their cell cycle distribution. Analysis of donor-derived GFP⁺ cells revealed that $p27^{-/-}p57^{KD}$ LSK cells had a 2-fold decrease in the frequency of Ki67⁻ quiescent cells (Figure 4D) and a correlative increase in the percentage of BrdU⁺ cycling cells (Figure 4E). Thus, a proportion of quiescent LSK cells in the BM are profoundly affected by the loss of p57 when p27 is unavailable. Furthermore, examination of donor-derived GFP⁺ LSK cells after the second transplantation revealed a severe reduction in the self-renewal capacity of $p27^{-/-}p57^{KD}$ HSCs (Figure 4F).

Failure to Maintain Quiescence in $p27^{-/-}p57^{-/-}$ HSCs

Hematopoietic cells are rapidly expanded in the FL; however, FL EPCR⁺LSK cells are represented in a slow cycling population as early as E12.5 (Iwasaki et al., 2010). To confirm the genetic cooperation of p57 and p27 in regulating HSC proliferation, the cell cycle of E14.5 FL CD48⁻EPCR⁺LSK cells was examined in $p27^{-/-}p57^{-/-}$ (DKO) mice. Loss of both p27 and p57 significantly decreased the frequency of Ki67⁻ HSCs compared to the frequency in $p27^{-/-}$, $p57^{-/-}$, or WT mice (Figure S5A). However, no significant differences were detected in the total cell numbers of LSK and progenitors between DKO embryos and the other genotypes (Figure S5B). Furthermore, DKO FL CD48⁻EPCR⁺LSK cells showed no defects in colony formation after 7 days in methylcellulose culture (Figure S5C).

Next, the repopulation capacity of FL CD48⁻EPCR⁺LSK cells of various genotypes was examined after BMT. In the short-term (4 and 8 weeks post-BMT), the repopulating capacity of DKO donor-derived cells was comparable to that of other genotypes, and no alteration was observed to suggest that loss of p27 and p57 affects progenitor function (Figure 5A). However, at later time points, the repopulating capacity of DKO cells was lower than that of the control groups. In addition, the number of DKO donor-derived LSK cells sharply decreased at 4 months post-BMT (Figure 5B). These results indicate that deficiency of p27 and p57 may affect the function of HSCs but not that of progenitor cells. In fact, there was a significant reduction in the frequency of CD48⁻CD150⁺LSK cells in reconstituting DKO BM compared to that in controls (Figure 5C). This decrease was not associated with changes in the apoptotic rates of these cells (data not shown).

Based on these observations, the cell cycle profile of reconstituting subpopulations of HSCs (CD48⁻CD150⁺LSK cells) and HPCs (CD48⁺LSK cells) was further tested. DKO HSCs, while decreased in number, displayed enhanced proliferation, while DKO HPCs did not cycle more than the control groups (Figure 5D). On the other hand, flow cytometric analyses identified

an increased number of myeloid (Mac-1⁺ and Gr-1⁺) cells as well as a reduction in the number of B (B220⁺) cells in DKO donor-derived BM cells; in contrast, an increased number of T (CD4⁺CD8⁺) cells was detected in both $p27^{-/-}$ and DKO cells (Figure 5E). Despite the perturbed frequency of HSCs and various hematopoietic cell lineages in reconstituting DKO BM, no significant extramedullary hematopoiesis was detected because the spleen size and the frequency of splenic LSK cells in DKO cell recipients were similar to those in other genotypic cell recipients (Figure S5D and data not shown). Specifically, the deficiency of both p57 and p27 in HSCs resulted in a complete lack of long-term maintenance of HSCs after serial BMT (Figure 5F), suggesting that these proteins cooperate to play a pivotal role in the maintenance of HSC quiescence and to protect HSCs from loss of self-renewal activity.

Identification of Hsc70 as a p57 Binding Protein in Quiescent Hematopoietic Cells

Given our *in vivo* studies suggesting that p57 and p27 cooperate to maintain quiescence in HSCs, p57/p27 binding factors were investigated to elucidate the mechanism of this cooperation. Murine EML cells, a hematopoietic progenitor cell line, were used to identify p57 binding proteins. As previously reported (Ye et al., 2005), lineage⁻ EML cells can be separated into two populations based on the cell surface marker CD34, and both populations contain similar levels of c-kit. In addition, it was found that the CD34⁺ population was active in cell cycling, whereas the CD34⁻ cells were in G₀/G₁ cell cycle arrest, as indicated by Ki67 staining (Figure 6A). It was also observed that p57 was expressed at high levels in CD34⁻EML cells, while increased c-Myc was detected in CD34⁺EML cells, correlating with the cell cycle status (Figure S6A).

To identify proteins that physically associate with p57 in quiescent EML cells, p57 binding proteins were coimmunoprecipitated on anti-Myc agarose beads from whole cell extracts of Lin⁻CD34⁻ EML cells overexpressing Myc-p57. Several proteins coprecipitated with Myc-p57 that were absent in the control purification (Figure 6B). Protein bands were excised, digested with trypsin, and subjected to Nano-liquid Chromatography-Tandem Mass Spectrometry (LC-MS/MS). Cyclin D1, D2, CDK4, and CDK6 were identified as prominent copurifying proteins. In addition, the mass spectra identified several tryptic peptides that were identical to murine Hsc70. Also, Hsc70 was detected as an endogenous binding protein of p57 by immunoprecipitation with p57- or Hsc70-specific antibodies in Lin⁻CD34⁻ EML cell lysates (Figure 6C).

Hsc70 is a member of the heat shock protein 70 (Hsp70) family, which shuttles between the cytoplasm and the nucleus and serves as a molecular chaperone for the nuclear import of certain proteins. Diehl et al. (2003) showed that Hsc70 directly

(D) Defective maintenance of quiescence in $p27^{-/-}p57^{KD}$ LSK cells. Cell cycle analysis of GFP⁺ donor-derived LSK cells was performed by staining with Hoechst and Ki67 at 16 weeks post-BMT. Inserts show the mean percentages (\pm SD) of donor-derived GFP⁺ LSK cells ($^*p < 0.01$, $n = 5$).

(E) Increased BrdU⁺ cells in $p27^{-/-}p57^{KD}$ LSK cells. Recipient mice were intraperitoneally injected with 1 mg of BrdU at 16 weeks post-BMT. Twenty-four hours after injection, BM MNCs were harvested and stained with surface markers and BrdU antibodies and then analyzed by flow cytometry. The percentages (\pm SD) of BrdU⁺ cells in donor-derived LSK cells are indicated ($^*p < 0.01$, $n = 5$).

(F) Defective repopulation capacity of $p27^{-/-}p57^{KD}$ LSK cells in second BMT. Donor-derived GFP⁺ LSK cells (5×10^3) were obtained from recipient mice and transplanted into sublethally irradiated mice. Data shown are the mean percentages (\pm SD) of donor-derived GFP⁺ LSK cells at 16 weeks after the second BMT ($^*p < 0.01$, $n = 5$).

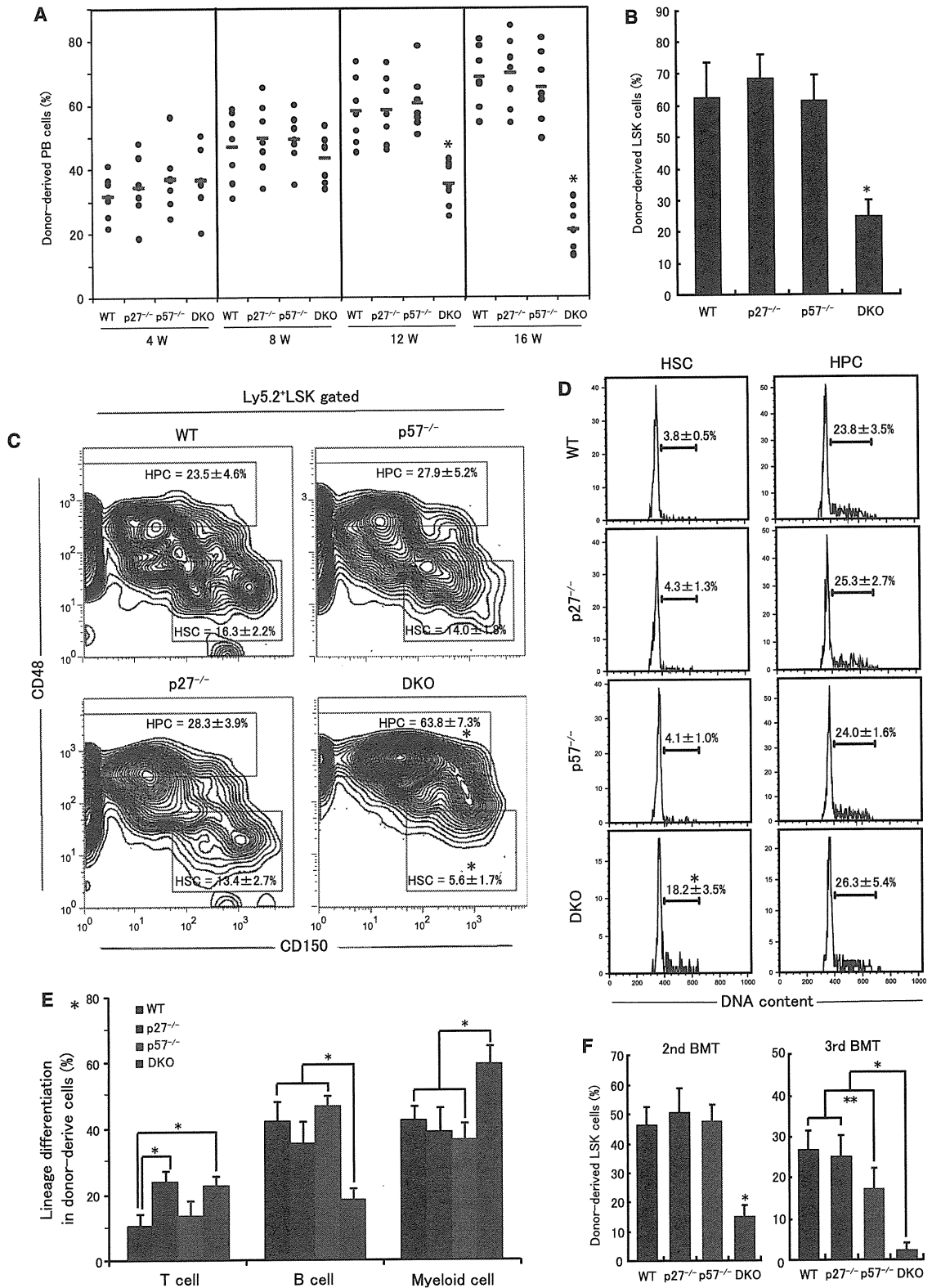


Figure 5. Defects in the Maintenance of Quiescence and the Self-Renewal Capacity of *p27^{-/-}p57^{-/-}* HSCs

(A) Defective hematopoietic repopulating activity of DKO FL HSCs. 5×10^2 FL CD48⁻EPCR⁺LSK cells from WT, *p27^{-/-}*, *p57^{-/-}*, or DKO mice were transplanted into irradiated recipients together with 2×10^5 BM-MNC competitors. Red lines indicate the mean percentages of donor-derived PB cells (* $p < 0.01$, $n = 7$).

interacts with cyclin D1 and accelerates its binding to CDK4/6 during the G_0/G_1 -S transition. Hsc70 is constitutively expressed in the absence of stress in mature mammalian cells and is abundantly expressed in embryonic, mesenchymal, and neural stem cells (Baharvand et al., 2007). The relative levels of Hsc70 mRNA were examined in hematopoietic cells, and Hsc70 was found to be highly expressed in multipotent LSK cells (Figure S6B). In contrast, Hsp70-1a, a member of the Hsp70 family whose expression is induced by stressors such as heat, is expressed at low levels in LSK cells (Figure S6C). The subcellular localization of cyclin D1 and Hsc70 in CD34⁻LSK cells was next analyzed by immunocytochemistry. Cyclin D1 colocalized with Hsc70 in the cytoplasm of untreated CD34⁻LSK cells but translocated into the nucleus with Hsc70 after SCF stimulation (Figure S6D). These results suggest that the localization of Hsc70 to the cytoplasm of HSCs may inhibit the G_0/G_1 -S transition by regulating the subcellular localization of cyclin D1.

To determine whether other CDK inhibitors bind to Hsc70, expression vectors encoding EGFP-tagged Hsc70 and HA-tagged p21, p27, or p57 were cotransfected into COS-7 cells. EGFP-Hsc70 was immunoprecipitated with anti-GFP from the cell lysates, and immunoblotting was carried out with HA or GFP antibodies. HA-p57 and HA-p27, but not HA-p21, coprecipitated with EGFP-Hsc70 (Figure 6D), suggesting that p57 and p27 may specifically interact with Hsc70 to regulate cell cycle progression in HSCs. Consistent with this, the hyperphosphorylation of Rb in DKO HSCs correlated with the nuclear import of the Hsc70/cyclin D1 complex in donor-derived CD34⁻LSK cells (Figure 6E). These observations suggest that loss of p57 and p27 in HSCs results in Rb phosphorylation and causes cell cycle entry by regulating the nuclear import of the Hsc70/cyclin D1 complex.

Control of the Cytoplasmic Hsc70/Cyclin D1 Complex Is a Key Molecular Mechanism of HSC Quiescence

Deoxyspergualin (DSG), an immunosuppressive agent, has a peptidomimetic structure and binds specifically to Hsc70, which is thought to preclude the binding of certain other proteins to Hsc70 (Nadler et al., 1992). Immunoprecipitation assays were performed in the presence or absence of DSG to identify the interactions between Hsc70, p57, and cyclin D1 proteins in Myc-p57- or cyclin D1-overexpressing Lin⁻CD34⁻ EML cells. Hsc70 bound to both p57 and cyclin D1, but DSG only inhibited the association between Hsc70 and cyclin D1 (Figure 6F). When freshly isolated BM CD34⁻LSK cells were treated with DSG to inhibit the binding of Hsc70 to cyclin D1, cyclin D1 was imported into the nucleus and Rb became phosphorylated, whereas Hsc70 remained localized to the cytoplasm (Figure S6E). These data suggest that Hsc70 maintains the cytoplasmic localization

of cyclin D1 through direct binding and functions as a specific G_0/G_1 factor relative to Rb phosphorylation in HSCs.

A nuclear localization signal (NLS) and a nuclear localization-related signal (NLRS) have been identified in amino acid regions 246–262 and 473–492, respectively, of Hsc70 (Tsukahara and Maru, 2004). Blocking of the NLRS, which functionally inhibits the nuclear export signal (NES), results in the inhibition of Hsc70 nuclear translocation (Figure S7A). GFP fusions were constructed of WT or NLRS-deficient (NLRS-D) Hsc70, which also binds to cyclin D1 (Figure S7B), and their subcellular localizations were examined in COS7 cells. WT Hsc70 localized to both the cytoplasm and the nucleus at 37°C and accumulated in the nucleus after heat shock at 42°C for 4 hr. In contrast, NLRS-D Hsc70 remained exclusively in the cytoplasm (Figure S7C).

Given that the nuclear translocation of Hsc70 was altered by the deletion of the NLRS, cell cycle progression was next compared in HSCs overexpressing WT or NLRS-D Hsc70. There was no significant difference in cell cycle status in culturing GFP⁺LSK cells transduced with WT Hsc70 or NLRS-D Hsc70, compared to cells transduced with the GFP control vector (Figure S7D). We next examined the proliferation of the transduced cells 8 weeks after BMT. Analysis of the reconstituting BM showed an increase in the LSK fraction and a decrease in the CD34⁻LSK cell population in mice transplanted with cells transduced with WT Hsc70. Ki67 staining showed that the percentage of G_0 cells in repopulating CD34⁻LSK cells was significantly decreased by WT Hsc70, whereas deletion of the Hsc70 NLRS prevented the reduction in the number of Ki67⁻ cells (Figure 7A). Furthermore, analysis of the donor-derived GFP⁺CD34⁻LSK fraction showed that a significant increase in the percentage of BrdU⁺ cells occurred in WT Hsc70-transduced cells but not in NLRS-D Hsc70- or control vector-transduced cells (Figure 7B). In addition, donor-derived CD34⁻LSK formed few colonies in WT Hsc70- but not in NLRS-D Hsc70-transduced cohorts (Figure 7C). These data demonstrate that the subcellular localization of Hsc70 is critical for the maintenance of HSC cell cycle kinetics and repopulating capacity after BMT.

To examine the role of CDKs in these processes, the effect of the pharmacologic inhibition of CDK4/6 (with PD-0332991) or CDK2 (with BMS-387032) was evaluated in mice transplanted with HSCs overexpressing WT or NLRS-D Hsc70. Treatment in vivo with PD-0332991 significantly induced G_0 quiescence in HSCs expressing WT Hsc70, whereas BMS-387032 treatment increased the frequency of the G_1 population. In contrast, neither PD-0332991 nor BMS-387032 significantly affected the frequency of G_0 or G_1 cells in NLRS-D Hsc70-overexpressing HSCs, though the S/ G_2 /M population was slightly suppressed by BMS-387032 in these cells (Figure 7D). In addition, CD34⁻LSK cells were isolated from WT or DKO donor-derived

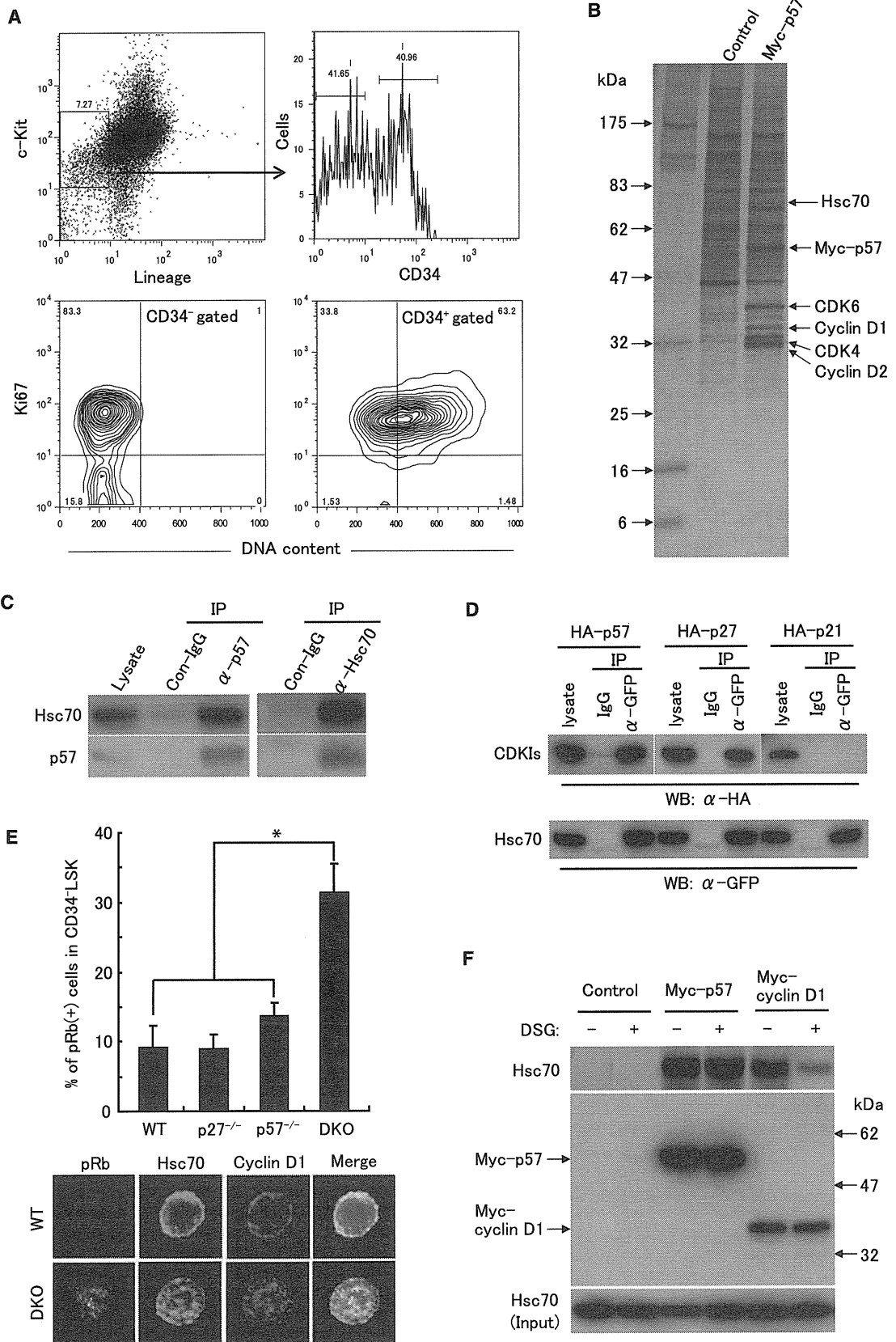
(B) Defective LSK repopulating activity of DKO cells. BMT experiments were performed as in (A). Data shown are the mean percentages (\pm SD) of donor-derived LSK cells at 16 weeks post-BMT (* $p < 0.01$, $n = 7$).

(C) Flow cytometric analysis of donor-derived BM fractions. The frequency of CD48⁻CD150⁺LSK cells was significantly reduced in reconstituting DKO BM as compared to other controls. Inserts shown are the mean percentages (\pm SD) of donor-derived LSK cells (* $p < 0.01$, $n = 7$).

(D) Proliferation status in donor-derived HSC and HPC populations. The cell cycle status of HSCs (CD48⁻CD150⁺LSK cells) or HPCs (CD48⁺LSK cells) was determined by intracellular Hoechst staining. The mean percentage \pm SD of cells in S/ G_2 /M is indicated (* $p < 0.01$, $n = 7$).

(E) The percentage (\pm SD) of CD4/CD8⁺ T cells, B220⁺ B cells, or Mac-1⁺/Gr-1⁺ myeloid cells of donor-derived BM cells in BMT recipients (* $p < 0.01$, $n = 7$).

(F) Defective repopulating capacity of DKO LSK cells during serial BMT. The percentages (\pm SD) of donor-derived LSK cells were determined at 16 weeks after the second and third BMT (* $p < 0.01$, ** $p < 0.05$, $n = 4$).



BM at 4 months post-BMT. After 12 hr of culture with low-dose SCF (10 ng/ml) and with or without DSG, PD-0333991, and BMS-387032, cell cycle initiation was determined by Ki67 staining (Figure S7E). Treatment with PD-0332991 blocked the cell cycle progression induced by p27 and p57 deletion, whereas BMS-387032 had no effect on DKO cells. These data demonstrate that the CDK4/6 activity elicited by the nuclear expression of Hsc70/cyclin D1 releases HSCs from p27/p57-protecting quiescence. This model is additionally supported by the requirement for CDK4/6 but not CDK2 for cell cycle entry after DSG stimulation (Figure S7E).

DISCUSSION

Here, we report that the CDK inhibitors p57 and p27 cooperate to maintain HSC quiescence and that their function is closely correlated to the regulation of the cellular localization of the Hsc70/cyclin D1 complex in HSCs (Figure 7E).

Loss of p57 in FL HSCs Leads to Impaired Self-Renewal in Serial BMT, although the HSC Cell Cycle Is Not Affected

Upon mitogenic stimuli, D-type cyclins phosphorylate Rb, initiating G₀/G₁-S phase progression. Interestingly, HSCs abundantly express cytoplasmic cyclin D1, which is essential for HSC proliferation (Kozar et al., 2004) and which is correlated with the high expression of p57 in the cytoplasm of quiescent HSCs. In addition, SCF downregulates p57 and induces the nuclear translocation of cyclin D1 in HSCs (Figure S1). These findings suggest that, in quiescent HSCs, p57 and cyclin D1 form a complex in the cytoplasm and cyclin D1 is available for rapid re-entry into the cell cycle in response to mitogenic signals. Recent studies have indicated that the cytoplasmic localization of cyclin D1 plays an important role in cell cycle control (Tamura-Adachi et al., 2003; Yamamoto et al., 2006). In addition, evidence for the cytoplasmic localization of p57 has been provided in normal and cancerous tissues (Pateras et al., 2009). Although a similar expression pattern has been reported for HSCs (Yamazaki et al., 2006), the exact functions of p57 are still not known.

The function of p57 was first examined with FL HSCs because p57-null mice show neonatal lethality. Unexpectedly, there were

no significant abnormalities in the function of p57^{-/-} HSCs, although a defect in repopulating capacity was observed in serial BMT. Moreover, no defects were detected in the cell cycle control of p57^{-/-} donor-derived LSK cells, indicating the presence of alternative mechanisms to maintain quiescence (Figure 2). Interestingly, in the p57^{-/-} donor-derived LSK cells, the levels of p27 and p18 were increased significantly, indicating that these proteins may functionally compensate for p57 in the maintenance of HSC quiescence. However, after administration of THPO to transplant recipient mice, the p18 level remained unchanged, whereas p27 expression was elevated in p57^{-/-} LSK cells. Furthermore, the expression of p27 but not p18 in the cytoplasm of p57^{-/-} HSCs was similar to that of p57 in WT HSCs, suggesting compensation for the lack of p57 by p27 (Figure 3). Indeed, p18 has been reported to play a negative role in self-renewal through an independent mechanism of cell cycle arrest in HSCs (Yuan et al., 2004). These findings suggest that p57 deficiency induces the exhaustion of HSCs after repeated BMTs by upregulating p18, and not defective HSC quiescence by p27 compensation. It remains to be determined why p57 deletion increases p18 during serial BMT and, more importantly, how p27 is functionally upregulated by p57 deletion to maintain HSC quiescence.

p57 and p27 Cooperate to Maintain Cell Cycle Quiescence and the Reconstitution Activity of HSCs

Both p27 and p57 have broad antiproliferative effects on a variety of cell types and tissues outside the hematopoietic system. Previous studies with mice lacking p27 and p57 have shown that these proteins cooperate to control the cell cycle in many tissues (Bilodeau et al., 2009; Zhang et al., 1998). In addition, it was demonstrated that p57 and p27 have overlapping functions in a knockin mouse model (Susaki et al., 2009). However, the physiological significance and the molecular mechanism for the cooperation between p27 and p57 in stem cells were not evaluated in previous studies.

In this study, the deficiency of both p57 and p27 resulted in a complete lack of long-term maintenance of HSCs, suggesting that these proteins cooperate to maintain HSC quiescence and protect HSCs from a loss of self-renewal activity (Figures 4 and 5). We have previously reported that Foxo3a, an important downstream target of PI3K-Akt signaling, is essential for the

Figure 6. Association of Hsc70 with p57, p27, and Cyclin D1

(A) Cell cycle analysis of CD34⁻ and CD34⁺Lin⁻ EML cells. Cells were stained with c-kit, CD34, and lineage (CD4, CD8, B220, TER-119, Gr-1, Mac-1) antibodies and analyzed by anti-Ki67 staining. Bottom panels indicate the cell cycle pattern of CD34⁻ and CD34⁺Lin⁻ EML cells.

(B) Detection of p57-associated proteins by mass spectrometry. The left lane contains molecular weight markers (sizes shown in kilodaltons), the middle lane contains proteins that nonspecifically bind to anti-myc beads in control EML lysates, and the right lane contains p57 complexes isolated from lysates from Myc-p57-infected EML cells. The positions of cyclin D1, cyclin D2, CDK4, CDK6, Myc-p57, and Hsc70 are indicated, along with the peptides identified by mass spectrometry.

(C) Hsc70 was detected in the p57 endogenous complex. Lin⁻CD34⁻ EML cell lysates were immunoprecipitated with p57- or Hsc70-specific antibodies, and the bound complexes were immunoblotted for p57 or Hsc70.

(D) Hsc70 directly binds to p57 and p27. Expression vectors encoding EGFP-tagged Hsc70 and HA-tagged p21, p27, or p57 were cotransfected into COS-7 cells. EGFP-Hsc70 was immunoprecipitated with anti-GFP, and immunoblotting was carried out with HA or GFP antibodies.

(E) The phosphorylation of Rb is increased in p27^{-/-}p57^{-/-} HSCs. p27^{-/-}p57^{-/-} donor-derived CD34⁺LSK cells were isolated by FACS at 16 weeks post-transplantation and stained with anti-Hsc70 (green), anti-cyclin D1 (red), anti-pRb (white), and DAPI (blue). Data shown are the mean (±SD) values from two independent experiments (*p < 0.01).

(F) DSG inhibits the association between Hsc70 and cyclin D1. EML cells were infected with Myc-p57 or Myc-cyclin D1 retroviruses and were cultured in the presence or absence of 10 μg/ml DSG for 24 hr. Immunoprecipitation with Myc antibodies was performed on the infected Lin⁻CD34⁻ EML cells, and immunoblotting was carried out with Hsc70 or Myc antibodies.

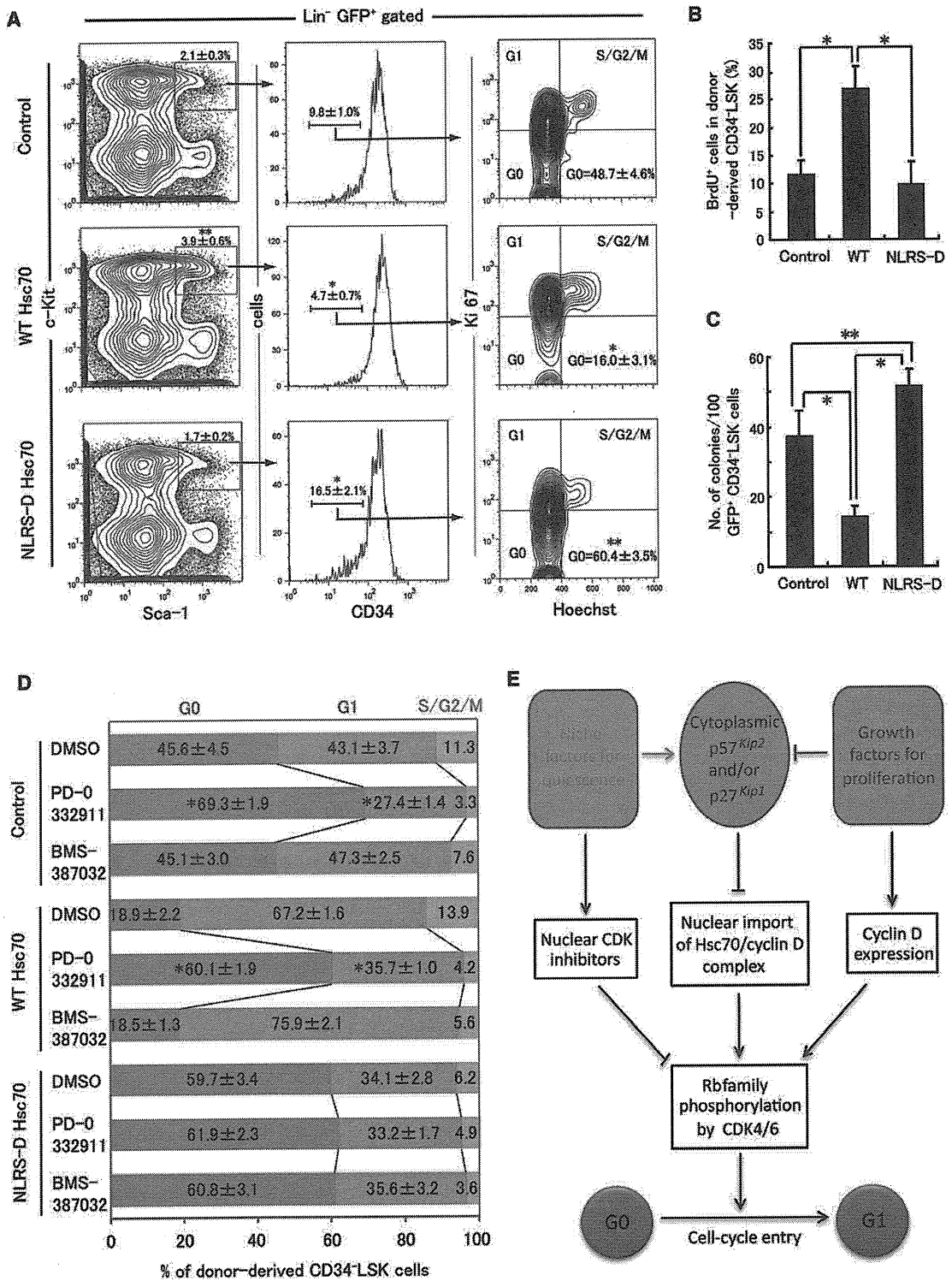


Figure 7. Control of Cytoplasmic Hsc70/Cyclin D1 Localization Is a Key Molecular Mechanism of HSC Quiescence

(A) Cell cycle analysis of donor-derived WT Hsc70 and NLR5-D Hsc70-transduced CD34⁻LSK cells at 2 months after BMT. Inserts shown are the mean percentages (±SD) of donor-derived CD34⁻LSK cells (*p < 0.01, **p < 0.05, n = 4).

(B) Increased frequency of BrdU⁺ cells in the donor-derived WT-Hsc70 and NLR5-D Hsc70-transduced CD34⁻LSK cells at 2 months after BMT. Recipient mice were intraperitoneally injected with 1 mg of BrdU at 2 months post-BMT. Twenty-four hours after injection, BM MNCs were harvested and stained with surface marker and BrdU antibodies and then analyzed by flow cytometry. The percentages (±SD) of BrdU⁺ cells in donor-derived CD34⁻LSK cells are indicated (*p < 0.01, n = 4).

maintenance of self-renewal capacity in HSCs. Maintenance of quiescence is defective in *Foxo3a*^{-/-} HSCs, concomitant with the decreased expression of both p57 and p27 (Miyamoto et al., 2007). Another genetic model that illustrates the relationship between the PI3K-Akt pathway and HSC quiescence is the conditional knockout of PTEN, which regulates HSC maintenance by restricting HSC proliferation (Yilmaz et al., 2006; Zhang et al., 2006). The deficiency leads to the activation of PI3K, which results in Akt activation and consequently Foxo inactivation. This relationship may explain the similarities in the phenotypes of *PTEN*^{-/-}, *Foxo3a*^{-/-}, and *p27*^{-/-}*p57*^{-/-} HSCs with respect to cell cycle regulation and repopulating capacity. More interestingly, the PI3K pathway also plays an important role in controlling the localization of cytoplasmic cyclin D1 in various cell lines (Radu et al., 2003; Yamamoto et al., 2006). These findings are especially interesting to us as the PI3K-Akt pathway acts upstream of p57 and p27 to control cyclin D1 localization in HSCs. The fact that both p57 and p27 function downstream of the same regulatory pathway may well be important. One possible explanation is that this compensatory mechanism exists to ensure that the cell cycle regulatory function of the PI3K pathway is intact even if one effector becomes inactivated.

Increased proliferation is often associated with the loss of self-renewal in HSCs, and alterations in the downstream regulators (Rb family members) of the CDK inhibitors are also associated with this phenotype (Viatour et al., 2008). Rb family proteins collectively regulate genes that normally inhibit the proliferation of both HSCs and hematopoietic progenitors. In contrast, p27 and p57 deficiency resulted in an altered cell cycle for HSCs but not for progenitors. These observations suggest that the cell cycle progression of HSCs and progenitors may be controlled by different mechanisms, although both processes are regulated by the Rb gene family.

Taken together, our results indicate that either p57 or its compensator p27 specifically plays a pivotal role in controlling HSC quiescence. This compensatory mechanism of p27 may provide an essential proliferation control in stem cells where p57 is not expressed at normal levels, as is the case in many human tumors and hyperplasia.

Importance of Hsc70, a p57 and p27 Binding Protein, in the Regulation of HSC Quiescence

Hsp70/Hsc70 chaperones localize to both cytosolic and nuclear compartments, where they regulate protein maturation, translocation, and association. Previous studies have shown that Hsp70 prevents the inactivation of the transcription factor GATA-1 by a caspase-mediated proteolysis, indicating that Hsp70 might indirectly trigger erythroid differentiation (Ribeil et al., 2007). Hsc70 also plays a role in the cytokine-mediated survival of hematopoietic progenitors by negatively influencing

the stability of mRNA of the proapoptotic protein Bim, thus preventing apoptosis in hematopoiesis and leukemogenesis (Matsui et al., 2007). However, neither molecule has been shown to play a specific role in HSCs.

In this study, Hsc70 was identified as a p57 binding protein under quiescent conditions with the Lin⁻CD34⁻EML cells. Hsc70 is also associated with p27 and is involved in cell cycle progression (Figure 6D; Imamura et al., 2009). Moreover, Diehl et al. (2003) demonstrated that Hsc70-cyclin D1 binding can stabilize cyclin D1 and regulate its transport into the nucleus. Interestingly, Hsc70 and cyclin D1 formed a complex and additionally colocalized in the cytoplasm of quiescent HSCs. In future studies, identification of the stoichiometry of the p57/p27-Hsc70-cyclin D1 complex could help further investigations into the roles of these proteins in various contexts.

To determine whether the nuclear translocation of Hsc70 is functionally involved in the control of HSC quiescence, the cell cycle status of CD34⁻LSK cells transduced with WT Hsc70 or NLR5-D Hsc70 were examined. The percentage of G₀ cells in WT Hsc70-transduced cells was significantly decreased and, interestingly, this effect was restored by the administration of a CDK4/6 inhibitor (PD-0332911) but not a CDK2 inhibitor (BMS-387032) (Figure 7). These results indicate that the subcellular localization of Hsc70, which regulates the activity of CDK4/6 by controlling the localization of cyclin D1, potentially acts downstream of p57 and p27 to control the quiescence of HSCs. Consistent with these observations, the enhanced proliferation of DKO HSCs compared to WT or single knockout HSCs is, at least in part, mediated by the nuclear import of the Hsc70/cyclin D1 complex (Figure 6E). Further, the treatment of HSCs with PD-0332911 blocked cell cycle progression induced by p27 and p57 deletion, whereas BMS-387032 had no effect on DKO cells. Collectively, our data suggest that p57 and p27 may regulate the activity of CDK4/6 by controlling the cellular localization of cyclin D1 through the association with Hsc70, resulting in the maintenance of HSC quiescence.

DSG, an Hsc70-binding immunosuppressive agent, inhibited the association between Hsc70 and cyclin D1 and resulted in the nuclear accumulation of cyclin D1 in HSCs, accompanied by Rb phosphorylation (Figure S6E). This finding further suggests that the appropriate distribution of cyclin D1 between the nucleus and cytoplasm is regulated by Hsc70 and is closely associated with cell cycle progression in HSCs. In addition, treatment with DSG in mice showed a potent BM suppression accompanying cyclin D1 degradation (data not shown), suggesting that the immunosuppressive properties of DSG are due, at least in part, to the disruption of the Hsc70-cyclin D1 interaction in BM cells.

Hsc70 has been considered to be a potential target in stem cell-based therapy. Expression of Hsc70, which is important

(C) Defective clonogenic capacity of donor-derived WT Hsc70-transduced CD34⁻LSK cells HSCs in vitro. Donor-derived GFP control-, WT Hsc70-, or NLR5-D Hsc70-transduced CD34⁻LSK cells were sorted at 2 months post-BMT and cultured in methylcellulose medium for 7 days. Data shown are the mean number of colonies (±SD) formed per 100 cells (*p < 0.01, **p < 0.05, n = 3).

(D) Cell cycle analysis of donor-derived GFP control-, WT Hsc70-, or NLR5-D Hsc70-transduced CD34⁻LSK cells after administration of pharmacologic CDK inhibitors in vivo. Recipient mice were intraperitoneally injected with 100 mg/kg of PD-0332911 or BMS-387032 at 2 months post-BMT. Twenty-four hours after injection, BM MNCs were harvested and cell cycle progression was analyzed as in (A). The percentages (±SD) of G₀, G₁, and S/G₂/M phase cells in donor-derived CD34⁻LSK cells are indicated (*p < 0.01, n = 3).

(E) Molecular regulation of the quiescence machinery in HSCs.

for the regulation of cyclin D1, is significantly upregulated in imatinib-resistant chronic myeloid leukemia (CML) cells (Pocaly et al., 2008). Furthermore, treatment with the Hsc70-specific inhibitor DSG in combination with imatinib decreases the viability of CML cells (José-Enériz et al., 2008). The slow cell cycle of leukemia stem cells may explain their resistance to anticancer drugs. Thus, the present study suggests that the manipulation of the cellular localization of Hsc70 and its binding to CDK inhibitors (p57 and p27) could serve as the basis for the development of new anticancer therapies.

EXPERIMENTAL PROCEDURES

Mice

Heterozygous *p57^{+/-}* or *p27^{+/-}* mice were crossed to generate *p57^{-/-}* or *p27^{-/-}* mice on a C57BL/6 background. C57BL/6 Ly5.1 congenic mice were purchased from Sankyo Lab Service (Tsukuba, Japan). Animal care was conducted in accordance with the guidelines of Keio University.

Flow Cytometry

Monoclonal antibodies (mAbs) recognizing the following markers were used for flow cytometric analyses and cell sorting (FACS Vantage or FACS Ariall, BD Bioscience): c-Kit (2B8), Sca-1 (E13-161.7), IL-7R α (SB/199), CD16/CD32 (2.4G2), Ki67 (B56), CD4 (RM4-5), CD8 (53-6.7), B220 (RA3-6B2), TER-119 (Ly-76), Gr-1 (RB6-8C5), CD34 (RAM34), CD41 (MWRReg30), CD48 (HM48-1), CD150 (TC15-12F12.2), CD45.1 (A20), CD45.2 (104), and anti-Mac-1 (M1/70). All mAbs were purchased from BD Biosciences. A mixture of mAbs recognizing CD4, CD8, B220, TER-119, Mac-1, and Gr-1 was used to identify Lin⁺ cells. For cell cycle analyses, FL or BM cells were collected and stained for LSK. Cells were then fixed with 4% paraformaldehyde in PBS and stained with Ki67 and Hoechst33342 (Molecular Probes).

Quantitative Real-Time RCR Analysis

qRT-PCR was performed on a 7500 Fast Real-Time PCR System with a TaqMan Fast Universal PCR master mixture (Applied Biosystems). Relative expression of the selected genes was normalized to that of β -actin (FAM4352933) for each sample. The following TaqMan Gene Expression Assay Mixes were used: cyclin D1 (Mm03053889_sl), cyclin D2 (Mm00438070_ml), cyclin D3 (Mm01612362_ml), cyclin E1 (Mm00432367_ml), cyclin E2 (Mm00438077_ml), *c-myc* (Mm00487803_ml), p18 (Mm00483243_ml), p21 (Mm00432448_ml), p27 (Mm00438167_gl), p57 (Mm01272135_gl), Hsc70 (Mm01731394_gH), and Hsp70-1a (Mm01159846_sl).

Immunocytochemistry

Immunocytochemistry was performed as previously described (Hosokawa et al., 2010). The following antibodies were used for immunocytochemistry: anti-p57, anti-p27 and anti-p18 (Santa Cruz); anti-Hsc70 and anti-Hsp70 (Stressgen); anti-cyclin D1 and anti-p21 (BD Pharmingen); and anti-pRb (Sigma). Nuclei were identified by staining with DAPI. For the inhibition experiments, HSCs were cultured with 10 μ g/ml DSG (Nippon Kayaku), 100 nM PD-0332991, or 100 nM BMS-387032 (Axon Medchem) before immunocytochemistry. Subcellular localizations were obtained with confocal laser scanning microscopy (FV1000, Olympus).

Mass Spectrometry

The LC-MS/MS analysis was performed as described previously (Sadaie et al., 2008).

Retroviral Transduction

Myc-p57, Myc-cyclin D1, and Hsc70 were ligated into the pMY-IRES-GFP vector, provided by Dr. Kitamura (University of Tokyo). Cyclin D1 cDNA was kindly provided by Dr. Ikeda (Tokyo Medical and Dental University). HA-p21, HA-p27, and HA-p57 in pcDNA3.1(+) vectors were kindly provided by Dr. Toyoshima (University of Tsukuba). Sequences of p57 shRNAs were as follows: sh-p57-1, 5'-GCAGGACGAGAATCAAGAG-3'; sh-p57-2, 5'-GAGAACTGCGCAGGAGAAC-3'; and sh-p57-3, 5'-CGACTTCTTCGCCAAGCGC-3'.

Each sequence was separated from the corresponding reverse complement of the same 19-nucleotide sequence by a 9-nucleotide noncomplementary spacer (TTCAAGAGA). A scrambled sequence (5'-GACACGCGACTTGTAC CAC-3') served as the negative control. Oligonucleotides were cloned into the BglII and HindIII sites of the pReGS retrovirus vector. To retrovirally transduce LSK cells, isolated *p27^{+/+}* or *p27^{-/-}* LSK cells were cultured for 2 days, transfected on RetroNectin (Takara Bio Inc.)-coated plates via Magnetofection (OZ Biosciences), according to the manufacturer's instructions, and then cultured for 2 additional days. Cultures were maintained in SF-O3 medium containing 1.0% BSA, 100 ng/ml SCF, and 100 ng/ml THPO.

Colony-Forming Assays

For LTC-IC, 3×10^3 GFP⁺LSK cells were cocultured with OP9 stromal cells, as previously described (Miyamoto et al., 2007). After 2–6 weeks in culture, cells were harvested and used in hematopoietic colony-forming assays.

Competitive Reconstitution Assay

Lethally irradiated C57BL/6 Ly5.1 congenic mice were reconstituted with FL-LSK cells from WT, *p27^{-/-}*, *p57^{-/-}*, or DKO mice (Ly5.2), in competition with BM MNCs from C57BL/6 Ly5.1 mice. For the serial transplantation analysis, donor-derived BM-LSK cells (4×10^3) were obtained from recipient mice at 16 weeks posttransplantation and transplanted into a second set of lethally irradiated mice. Subsequent transplantations were performed in the same manner.

Statistical Analysis

Significant differences between groups were determined with a two-tailed Student's *t* test.

SUPPLEMENTAL INFORMATION

Supplemental Information includes seven figures and can be found with this article online at doi:10.1016/j.stem.2011.07.003.

ACKNOWLEDGMENTS

This work was supported by a Grant-in-Aid for Scientific Research on Innovative Areas "Cancer Stem Cells" from the Ministry of Education, Culture, Sports, Science, and Technology (MEXT) of Japan, the Global COE program "Education and Research Center for Stem Cell Medicine" of Keio University, and a Grant-in-Aid for Japan Society for the Promotion of Science Fellows.

Received: August 13, 2010

Revised: February 15, 2011

Accepted: July 7, 2011

Published: September 1, 2011

REFERENCES

- Adolfsson, J., Borge, O.J., Bryder, D., Theilgaard-Mönch, K., Astrand-Grundström, I., Sitnicka, E., Sasaki, Y., and Jacobsen, S.E. (2001). Upregulation of Flt3 expression within the bone marrow Lin(-)Sca1(+)-kit(+/-) stem cell compartment is accompanied by loss of self-renewal capacity. *Immunity* 15, 659–669.
- Arai, F., Hirao, A., Ohmura, M., Sato, H., Matsuoka, S., Takubo, K., Ito, K., Koh, G.Y., and Suda, T. (2004). Tie2/angiopoietin-1 signaling regulates hematopoietic stem cell quiescence in the bone marrow niche. *Cell* 118, 149–161.
- Baharvand, H., Fathi, A., van Hoof, D., and Salekdeh, G.H. (2007). Concise review: Trends in stem cell proteomics. *Stem Cells* 25, 1888–1903.
- Bilodeau, S., Roussel-Gervais, A., and Drouin, J. (2009). Distinct developmental roles of cell cycle inhibitors p57Kip2 and p27Kip1 distinguish pituitary progenitor cell cycle exit from cell cycle reentry of differentiated cells. *Mol. Cell. Biol.* 29, 1895–1908.
- Cheng, T., Rodrigues, N., Dombkowski, D., Stier, S., and Scadden, D.T. (2000a). Stem cell repopulation efficiency but not pool size is governed by p27(kip1). *Nat. Med.* 6, 1235–1240.

- Cheng, T., Rodrigues, N., Shen, H., Yang, Y., Dombkowski, D., Sykes, M., and Scadden, D.T. (2000b). Hematopoietic stem cell quiescence maintained by p21cip1/waf1. *Science* 287, 1804–1808.
- Diehl, J.A., Yang, W., Rimerman, R.A., Xiao, H., and Emili, A. (2003). Hsc70 regulates accumulation of cyclin D1 and cyclin D1-dependent protein kinase. *Mol. Cell. Biol.* 23, 1764–1774.
- Hosokawa, K., Arai, F., Yoshihara, H., Iwasaki, H., Hembree, M., Yin, T., Nakamura, Y., Gomei, Y., Takubo, K., Shiama, H., et al. (2010). Cadherin-based adhesion is a potential target for niche manipulation to protect hematopoietic stem cells in adult bone marrow. *Cell Stem Cell* 6, 194–198.
- Imamura, Y., Fujigaki, Y., Oomori, Y., Usui, S., and Wang, P.L. (2009). Cooperation of salivary protein histatin 3 with heat shock cognate protein 70 relative to the G1/S transition in human gingival fibroblasts. *J. Biol. Chem.* 284, 14316–14325.
- Iwasaki, H., Arai, F., Kubota, Y., Dahl, M., and Suda, T. (2010). Endothelial protein C receptor-expressing hematopoietic stem cells reside in the perisinusoidal niche in fetal liver. *Blood* 116, 544–553.
- José-Enériz, E.S., Román-Gómez, J., Cordeu, L., Ballestar, E., Gárate, L., Andreu, E.J., Isidro, I., Guruceaga, E., Jiménez-Velasco, A., Heiniger, A., et al. (2008). BCR-ABL1-induced expression of HSPA8 promotes cell survival in chronic myeloid leukaemia. *Br. J. Haematol.* 142, 571–582.
- Kiel, M.J., Yilmaz, O.H., Iwashita, T., Yilmaz, O.H., Terhorst, C., and Morrison, S.J. (2005). SLAM family receptors distinguish hematopoietic stem and progenitor cells and reveal endothelial niches for stem cells. *Cell* 121, 1109–1121.
- Kozar, K., Ciemerych, M.A., Rebel, V.I., Shigematsu, H., Zagodzón, A., Sicinska, E., Geng, Y., Yu, Q., Bhattacharya, S., Bronson, R.T., et al. (2004). Mouse development and cell proliferation in the absence of D-cyclins. *Cell* 118, 477–491.
- Malumbres, M., Sotillo, R., Santamaría, D., Galán, J., Cerezo, A., Ortega, S., Dubus, P., and Barbacid, M. (2004). Mammalian cells cycle without the D-type cyclin-dependent kinases Cdk4 and Cdk6. *Cell* 118, 493–504.
- Matsui, H., Asou, H., and Inaba, T. (2007). Cytokines direct the regulation of Bim mRNA stability by heat-shock cognate protein 70. *Mol. Cell* 25, 99–112.
- Miyamoto, K., Araki, K.Y., Naka, K., Arai, F., Takubo, K., Yamazaki, S., Matsuoka, S., Miyamoto, T., Ito, K., Ohmura, M., et al. (2007). Foxo3a is essential for maintenance of the hematopoietic stem cell pool. *Cell Stem Cell* 1, 101–112.
- Nadler, S.G., Tepper, M.A., Schacter, B., and Mazzucco, C.E. (1992). Interaction of the immunosuppressant deoxyspergualin with a member of the Hsp70 family of heat shock proteins. *Science* 258, 484–486.
- Oguro, H., Iwama, A., Morita, Y., Kamijo, T., van Lohuizen, M., and Nakauchi, H. (2006). Differential impact of Ink4a and Arf on hematopoietic stem cells and their bone marrow microenvironment in Bmi1-deficient mice. *J. Exp. Med.* 203, 2247–2253.
- Passegué, E., Wagers, A.J., Giuriato, S., Anderson, W.C., and Weissman, I.L. (2005). Global analysis of proliferation and cell cycle gene expression in the regulation of hematopoietic stem and progenitor cell fates. *J. Exp. Med.* 202, 1599–1611.
- Pateras, I.S., Apostolopoulou, K., Niforou, K., Kotsinas, A., and Gorgoulis, V.G. (2009). p57KIP2: “Kip”ing the cell under control. *Mol. Cancer Res.* 7, 1902–1919.
- Pocaly, M., Lagarde, V., Etienne, G., Dupouy, M., Lapaillier, D., Claverol, S., Vilain, S., Bonneu, M., Turcq, B., Mahon, F.X., and Pasquet, J.M. (2008). Proteomic analysis of an imatinib-resistant K562 cell line highlights opposing roles of heat shock cognate 70 and heat shock 70 proteins in resistance. *Proteomics* 8, 2394–2406.
- Radu, A., Neubauer, V., Akagi, T., Hanafusa, H., and Georgescu, M.M. (2003). PTEN induces cell cycle arrest by decreasing the level and nuclear localization of cyclin D1. *Mol. Cell. Biol.* 23, 6139–6149.
- Ribeil, J.A., Zermati, Y., Vandekerckhove, J., Cathelin, S., Kersual, J., Dussiot, M., Coulon, S., Moura, I.C., Zeuner, A., Kirkegaard-Sørensen, T., et al. (2007). Hsp70 regulates erythropoiesis by preventing caspase-3-mediated cleavage of GATA-1. *Nature* 445, 102–105.
- Sadaie, M., Shinmyozu, K., and Nakayama, J. (2008). A conserved SET domain methyltransferase, Set11, modifies ribosomal protein Rpl12 in fission yeast. *J. Biol. Chem.* 283, 7185–7195.
- Scandura, J.M., Boccuni, P., Massagué, J., and Nimer, S.D. (2004). Transforming growth factor beta-induced cell cycle arrest of human hematopoietic cells requires p57KIP2 up-regulation. *Proc. Natl. Acad. Sci. USA* 101, 15231–15236.
- Susaki, E., Nakayama, K., Yamasaki, L., and Nakayama, K.I. (2009). Common and specific roles of the related CDK inhibitors p27 and p57 revealed by a knock-in mouse model. *Proc. Natl. Acad. Sci. USA* 106, 5192–5197.
- Tamamori-Adachi, M., Ito, H., Sumrejkanchanakij, P., Adachi, S., Hiroe, M., Shimizu, M., Kawachi, J., Sunamori, M., Marumo, F., Kitajima, S., and Ikeda, M.A. (2003). Critical role of cyclin D1 nuclear import in cardiomyocyte proliferation. *Circ. Res.* 92, e12–e19.
- Tsukahara, F., and Maru, Y. (2004). Identification of novel nuclear export and nuclear localization-related signals in human heat shock cognate protein 70. *J. Biol. Chem.* 279, 8867–8872.
- Viatour, P., Somerville, T.C., Venkatasubrahmanyam, S., Kogan, S., McLaughlin, M.E., Weissman, I.L., Butte, A.J., Passegué, E., and Sage, J. (2008). Hematopoietic stem cell quiescence is maintained by compound contributions of the retinoblastoma gene family. *Cell Stem Cell* 3, 416–428.
- Yamamoto, M., Tamakawa, S., Yoshie, M., Yaginuma, Y., and Ogawa, K. (2006). Neoplastic hepatocyte growth associated with cyclin D1 redistribution from the cytoplasm to the nucleus in mouse hepatocarcinogenesis. *Mol. Carcinog.* 45, 901–913.
- Yamazaki, S., Iwama, A., Takayanagi, S., Morita, Y., Eto, K., Ema, H., and Nakauchi, H. (2006). Cytokine signals modulated via lipid rafts mimic niche signals and induce hibernation in hematopoietic stem cells. *EMBO J.* 25, 3515–3523.
- Yamazaki, S., Iwama, A., Takayanagi, S., Eto, K., Ema, H., and Nakauchi, H. (2009). TGF-beta as a candidate bone marrow niche signal to induce hematopoietic stem cell hibernation. *Blood* 113, 1250–1256.
- Ye, Z.J., Kluger, Y., Lian, Z., and Weissman, S.M. (2005). Two types of precursor cells in a multipotential hematopoietic cell line. *Proc. Natl. Acad. Sci. USA* 102, 18461–18466.
- Yilmaz, O.H., Valdez, R., Theisen, B.K., Guo, W., Ferguson, D.O., Wu, H., and Morrison, S.J. (2006). Pten dependence distinguishes hematopoietic stem cells from leukaemia-initiating cells. *Nature* 441, 475–482.
- Yoshihara, H., Arai, F., Hosokawa, K., Hagiwara, T., Takubo, K., Nakamura, Y., Gomei, Y., Iwasaki, H., Matsuoka, S., Miyamoto, K., et al. (2007). Thrombopoietin/MPL signaling regulates hematopoietic stem cell quiescence and interaction with the osteoblastic niche. *Cell Stem Cell* 1, 685–697.
- Yuan, Y., Shen, H., Franklin, D.S., Scadden, D.T., and Cheng, T. (2004). In vivo self-renewing divisions of haematopoietic stem cells are increased in the absence of the early G1-phase inhibitor, p18INK4C. *Nat. Cell Biol.* 6, 436–442.
- Zhang, P., Wong, C., DePinho, R.A., Harper, J.W., and Elledge, S.J. (1998). Cooperation between the Cdk inhibitors p27(KIP1) and p57(KIP2) in the control of tissue growth and development. *Genes Dev.* 12, 3162–3167.
- Zhang, J., Grindley, J.C., Yin, T., Jayasinghe, S., He, X.C., Ross, J.T., Haug, J.S., Rupp, D., Porter-Westpfahl, K.S., Wiedemann, L.M., et al. (2006). PTEN maintains haematopoietic stem cells and acts in lineage choice and leukaemia prevention. *Nature* 441, 518–522.

p57 Is Required for Quiescence and Maintenance of Adult Hematopoietic Stem Cells

Akinobu Matsumoto,^{1,2} Shoichiro Takeishi,^{1,2} Tomoharu Kanie,^{1,2} Etsuo Susaki,^{1,2} Ichiro Onoyama,^{1,2} Yuki Tateishi,^{1,2} Keiko Nakayama,^{2,3} and Keiichi I. Nakayama^{1,2,*}

¹Department of Molecular and Cellular Biology, Medical Institute of Bioregulation, Kyushu University, 3-1-1 Maidashi, Higashi-ku, Fukuoka, Fukuoka 812-8582, Japan

²CREST, Japan Science and Technology Agency (JST), Kawaguchi, Saitama 332-0012, Japan

³Department of Developmental Genetics, Center for Translational and Advanced Animal Research, Graduate School of Medicine, Tohoku University, 2-1 Seiryō-machi, Aoba-ku, Sendai 980-8575, Japan

*Correspondence: nakayak1@bioreg.kyushu-u.ac.jp

DOI 10.1016/j.stem.2011.06.014

SUMMARY

Quiescence is required for the maintenance of hematopoietic stem cells (HSCs). Members of the Cip/Kip family of cyclin-dependent kinase (CDK) inhibitors (p21, p27, p57) have been implicated in HSC quiescence, but loss of p21 or p27 in mice affects HSC quiescence or functionality only under conditions of stress. Although p57 is the most abundant family member in quiescent HSCs, its role has remained uncharacterized. Here we show a severe defect in the self-renewal capacity of p57-deficient HSCs and a reduction of the proportion of the cells in G₀ phase. Additional ablation of p21 in a p57-null background resulted in a further decrease in the colony-forming activity of HSCs. Moreover, the HSC abnormalities of p57-deficient mice were corrected by knocking in the p27 gene at the p57 locus. Our results therefore suggest that, among Cip/Kip family CDK inhibitors, p57 plays a predominant role in the quiescence and maintenance of adult HSCs.

INTRODUCTION

Progression of the cell cycle is controlled by pairs of cyclins and cyclin-dependent kinases (CDKs). Progression through G₁ phase of the cell cycle is dependent on the cyclin D-CDK4 (or CDK6) complex, whereas cyclin E-CDK2 is required for the G₁-S transition and cyclins A and B together with CDK1 are required for G₂-M progression (Sherr and Roberts, 2004). Cell cycle progression is also under the control of negative regulators, the CDK inhibitors (CKIs), which belong to either the Ink4 or Cip/Kip families. Members of the Ink4 family—such as p16^{Ink4a}, p15^{Ink4b}, p18^{Ink4c}, and p19^{Ink4d}—are inhibitors specific for CDK4 or CDK6, whereas those of the Cip/Kip family, including p21^{Cip1} (p21), p27^{Kip1} (p27), and p57^{Kip2} (p57), mainly target CDK2 and CDK4 (and CDK1 in some situations) for inhibition.

Sustained hematopoiesis in adults requires preservation of a quiescent, multipotential hematopoietic stem cell (HSC) pool that intermittently yields progenitors with robust proliferative potential (Arai and Suda, 2007). In contrast, the cell cycle of

HSCs is active during embryogenesis in order to ensure expansion of the stem cell pool (Pawliuk et al., 1996). The ability of adult HSCs to reside in the quiescent state has been thought to be pivotal for maintenance of their “stemness.” However, the precise mechanisms by which such quiescence is established, maintained, and terminated have been largely unknown. CKIs including p21, p27, and p57 are implicated in the maintenance of quiescence, given their function to antagonize CDK activity that promotes cell proliferation. However, self-renewal of HSCs in mice deficient in p21 was found to be impaired only under stressful conditions in which DNA is damaged by exposure to 5-fluorouracil or γ -irradiation (Cheng et al., 2000b; van Os et al., 2007). Deletion of p27 in mice also does not affect the number, cycling, or self-renewal of HSCs (Cheng et al., 2000a). Although many studies have suggested the importance of p57 for maintenance of HSC stemness (Miyamoto et al., 2007; Qian et al., 2007; Yamazaki et al., 2006), the role of p57 in control of HSC quiescence has remained poorly characterized. Unlike p21- or p27-deficient mice, mice lacking p57 die immediately after birth, manifesting severe developmental defects (Takahashi et al., 2000; Yan et al., 1997; Zhang et al., 1997), which has rendered functional characterization of their HSCs technically difficult.

We have now established mice in which the p57 gene is conditionally disrupted in the hematopoietic system in order to avoid the neonatal mortality of conventional p57-deficient mice. Deletion of p57 alone, but not that of p21 or p27, resulted in a reduction in HSC number, in the size of the G₀ population, and in their reconstitution ability after transplantation. Mice lacking both p21 and p57 showed a more severe phenotype than those lacking p57 alone, and knockin of the gene for p27 at the p57 locus corrected the abnormalities of p57-deficient mice, suggestive of functional overlap between p57 and either p21 or p27. Our data thus indicate that p57 plays the dominant role among CKIs of the Cip/Kip family in maintenance of quiescence and stemness of HSCs.

RESULTS

p57 Is Predominantly Expressed in the Long-Term HSC Population

A previous study suggested that, among hematopoietic cells, p57 mRNA is most abundant in CD34^c-Kit⁺Sca-1⁺ lineage marker-negative (Lin⁻) HSCs (CD34^cKSL HSCs), a fraction with

long-term repopulating capacity (Yamazaki et al., 2006). In contrast, p21 mRNA was not detected in CD34⁻KSL HSCs, whereas p27 mRNA was found to be present in both CD34⁻KSL and CD34⁺KSL cells, the latter corresponding to a fraction with short-term repopulating capacity. To examine the expression of p57 in HSCs at the protein level, we performed immunoblot analysis of sorted bone marrow (BM) samples from 12 wild-type mice at 8 weeks of age. We sorted and fractionated KSL cells with the SLAM (signaling lymphocytic activation molecule) marker CD150. Similar to the pattern observed for its mRNA, p57 protein was most abundant in the CD150⁺KSL fraction, a fraction with long-term repopulating capacity; it was present in smaller amounts in the CD150⁻KSL fraction, a fraction with short-term repopulating capacity, and it was not detected in other fractions (Figure 1A). We did not detect p21 in any of the fractions tested, whereas p27 was expressed at a low level in the CD150⁺KSL and CD150⁻KSL populations. These patterns of protein expression prompted us to examine the effects of p57 ablation in HSCs.

Deletion of p57 Leads to a Reduction in Size of the HSC Population

Given that most conventional p57 knockout mice die during the perinatal period as a result of respiratory distress, probably caused by skeletal anomalies (Takahashi et al., 2000; Yan et al., 1997; Zhang et al., 1997), it has been technically difficult to characterize adult HSCs in such mice. We therefore established mouse embryonic stem cells (ESCs) that harbor a "floxed" p57 allele in which exons 2 to 4 (which include the entire coding region) are flanked by loxP sites (see Figure S1A available online). This allele was generated by homologous recombination followed by transient transfection of the ESCs with a vector for Cre recombinase in order to remove the introduced *neo* cassette (Figure S1B). Mice heterozygous for the floxed allele (*p57*^{+/-} mice) were generated by microinjection of the mutant ESCs into blastocysts and breeding of the resultant chimeric animals with mice of the C57BL/6 strain. The p57 locus undergoes genomic imprinting, with only the maternal allele being expressed (Matsuoka et al., 1995). The *p57*^{+/-} mice were indistinguishable from wild-type animals, confirming that the floxed allele is functional. We also confirmed that the phenotype of mice in which the maternal floxed allele was deleted by Cre recombinase expressed from the *Ella* gene promoter (Lakso et al., 1996) beginning early during embryogenesis was identical to that of conventional p57 knockout mice (Figure S1C). To ablate the maternal p57 allele only in the hematopoietic system, we crossed female *p57*^{+/-} mice with male mice harboring a Cre transgene under the control of the promoter for the myxovirus resistance 1 (Mx1) gene. We confirmed that almost all floxed alleles were inactivated by Cre recombinase in BM of Mx1-Cre/*p57*^{+/-} mice after intraperitoneal injection of poly(I)-poly(C) [poly(I:C)] to activate the Mx1 gene promoter (Figure S1D). Without poly(I:C) injection, a slight decrease in the abundance of p57 mRNA was observed in Mx1-Cre/*p57*^{+/-} mice compared with that in Mx1-Cre/*p57*^{+/+} mice. Deletion of the p57 allele resulted in a small increase in the amounts of p27 and p18 mRNAs in KSL cells, whereas deletion of p21 or p27 did not significantly affect the abundance of mRNAs for the corresponding other two CKIs (Figures S1E–S1H).

As early as 4 weeks after poly(I:C) injection, a substantial reduction in the size of the KSL fraction was apparent in p57-deficient mice compared with that in control littermates (Mx1-Cre/*p57*^{+/+} mice), which were also injected with poly(I:C) to exclude the possibility that poly(I:C) affected phenotype regardless of genotype (Figure 1B). This reduction in the size of the KSL fraction in p57-deficient mice was apparent for all KSL subpopulations examined (CD150⁻, CD150⁺CD48⁻, CD34⁻, or CD34⁺ cells) with the exception of CD150⁺CD48⁺ cells (Figure 1C). The total number and composition of cells in BM or peripheral blood were not otherwise affected by deletion of p57 at 4 weeks (Figures S1I–S1K and data not shown) or 4 months (Figure S1L and data not shown) after injection of poly(I:C), probably in part because the effect of such deletion in adult HSCs was compensated for at later stages of differentiation or had not had sufficient time to become manifest in the periphery within the period before analysis. In contrast, no reduction in the size of the HSC population was observed in p21- or p27-deficient mice (Figure 1C), consistent with the results of previous studies (Cheng et al., 2000a, 2000b; van Os et al., 2007). These findings thus suggested that p57 deletion affects the self-renewal capacity of HSCs.

Deletion of p57 Abrogates the Self-Renewal Capacity of HSCs

To assess the repopulating capacity of p57-deficient HSCs in vivo, we performed a competitive reconstitution assay in which BM cells (4×10^5) from poly(I:C)-injected Mx1-Cre/*p57*^{+/-} or Mx1-Cre/*p57*^{+/-} mice (CD45.2) competed against an equal number of BM cells from C57BL/6 heterozygous congenic mice (CD45.1/CD45.2) to reconstitute the hematopoietic compartment of irradiated C57BL/6 congenic mouse (CD45.1) recipients. At 16 weeks after BM cell transplantation (BMT), flow cytometric analysis of peripheral blood of the recipients revealed that the repopulating capacity of p57-deficient BM cells was markedly impaired, whereas that of *p21*^{-/-} or *p27*^{-/-} BM cells did not differ from that of cells from littermate controls (Figure 2A). Given that this result might have reflected the reduced number of HSCs in p57-deficient mice (Figures 1B and 1C), we also performed similar assays with total KSL cells (1.5×10^3) or CD150⁺CD48⁻KSL cells (2.0×10^2) isolated from p57-deficient mice or littermate controls at 4 weeks after poly(I:C) injection. The p57-deficient KSL cells showed a greatly impaired repopulating capacity after the first BMT, and this impairment was even more pronounced after a second BMT (Figures 2B and 2C). In addition, the frequency of KSL cells derived from p57-deficient donors among BM cells of the recipient mice was markedly smaller than that for KSL cells derived from control donors (Figure 2D). To determine whether p57 intrinsically regulates HSC repopulating capability, we transplanted BM cells (4×10^5) from either Mx1-Cre/*p57*^{+/-} mice or littermate controls not treated with poly(I:C) into lethally irradiated recipients together with the same number of competitor cells. After 4 weeks, we confirmed that donor cells were reconstituted in recipient BM and then injected the recipient mice with poly(I:C). Within 1 month after poly(I:C) injection, p57-deficient HSCs lost long-term repopulating capability and were eventually competed out by wild-type HSCs (Figure 2E), suggesting that a homing defect of transferred BM cells probably was not responsible for the impaired BM reconstitution by p57-deficient HSCs.

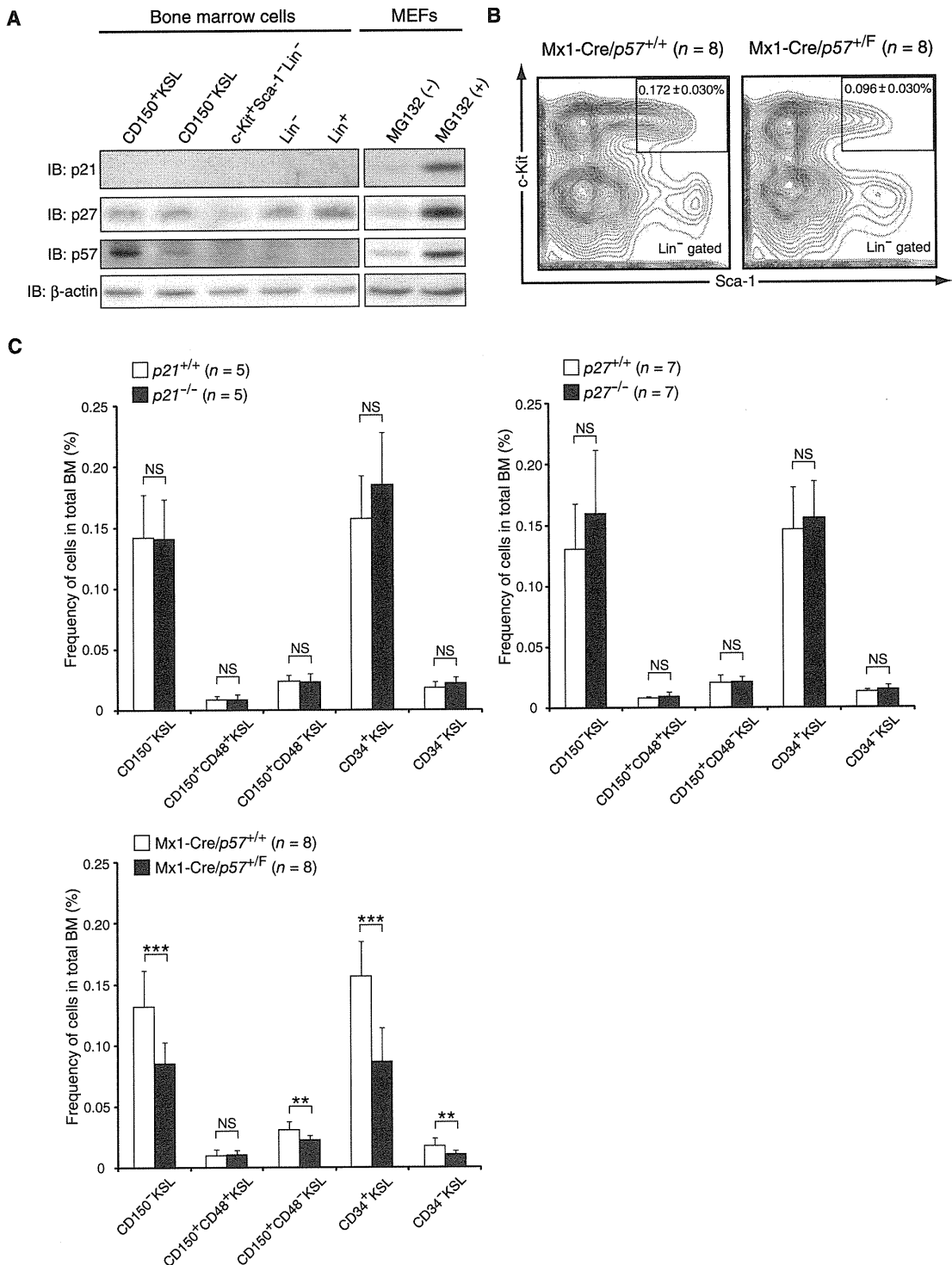


Figure 1. Decrease in HSC Number Induced by p57 Deletion

(A) Immunoblot analysis (IB) of fractionated hematopoietic cells from BM of wild-type mice. For positive and negative controls, mouse embryonic fibroblasts (MEFs) were cultured with or without 100 μ M MG132, respectively.

(B) Flow cytometric determination of the frequency of KSL cells among BM cells of Mx1-Cre/p57^{+/+} and Mx1-Cre/p57^{+/F} mice at 4 weeks after poly(I:C) injection. The percentages of KSL cells among total BM cells are shown as means \pm SD.

(C) Frequency of the indicated fractions among total BM cells from mice of the indicated genotypes. Mice harboring the Mx1-Cre transgene were examined at 4 weeks after poly(I:C) injection. Data are means \pm SD. ** $p < 0.01$, *** $p < 0.005$; NS, not significant.

See also Figure S1.

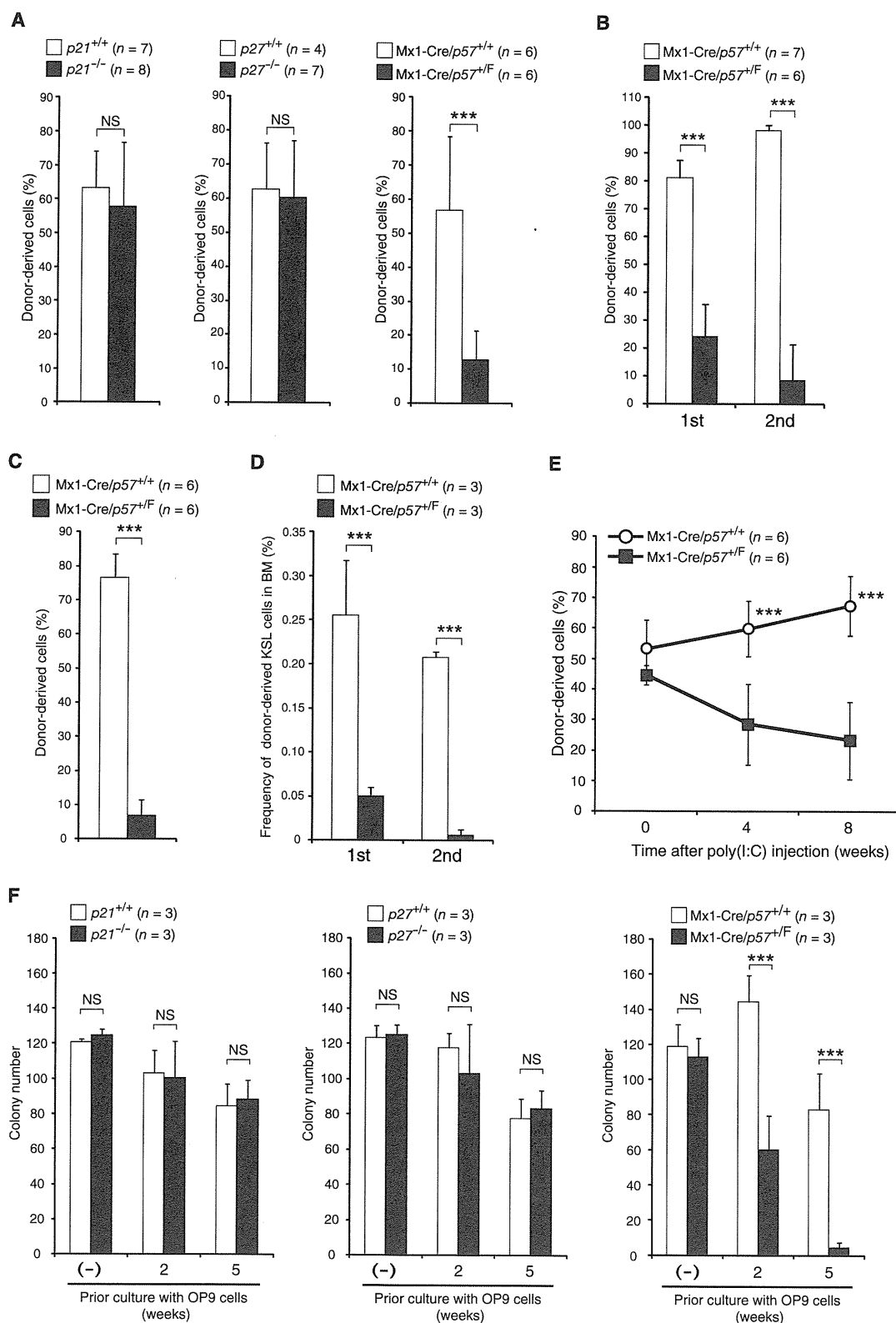


Figure 2. p57, but Not p21 or p27, Is Essential for HSC Maintenance

(A) Hematopoietic reconstitution capacity of BM cells (4×10^5) from donor mice of the indicated genotypes. Cells from donors harboring the Mx1-Cre transgene were harvested at 4 weeks after poly(I:C) injection. Data are means \pm SD. *** $p < 0.005$.

We further performed long-term culture of KSL cells on a layer of OP9 stromal cells, with the number of colony-forming cells arising after 2 or 5 weeks of culture reflecting the function of hematopoietic progenitor or stem cells, respectively. The number of colonies derived from p57-deficient KSL cells was significantly decreased compared with that derived from control cells, although a similar assay with freshly isolated KSL cells without culture did not show a significant difference in the number of colonies formed (Figure 2F). The number of colonies derived from p21- or p27-deficient KSL cells did not differ significantly from that derived from the corresponding control cells with or without culture on OP9 cells. A serial replating assay revealed that the number of colonies derived from p57-deficient KSL cells declined to a greater extent compared with that of colonies derived from control cells with each plating, whereas the number of colonies derived from p21- or p27-deficient KSL cells did not differ significantly from that derived from the corresponding control cells at each plating (Figure S2). Collectively, these results suggested that the self-renewal capacity of HSCs was profoundly affected by the loss of p57, but not by that of p21 or p27.

p57 Is Required for Maintenance of Quiescence in HSCs

HSCs are normally maintained in an undifferentiated quiescent (G_0 phase) state, with this quiescence protecting the cells against loss of self-renewal capacity. To evaluate directly HSC quiescence in p57-deficient mice, we stained KSL cells from poly(I:C)-injected Mx1-Cre/p57^{+/+} or Mx1-Cre/p57^{+/-} mice with a combination of Hoechst 33342 and pyronin Y, which differentially and quantitatively stain DNA and RNA and thereby allow detection of cells in G_0 phase. We found that 28% of control KSL cells were negative for staining with pyronin Y, indicative of normal HSC quiescence, whereas only 15% of p57-deficient KSL cells were in G_0 phase (Figures 3A and 3B). No such difference was observed for p21- or p27-deficient KSL cells and the corresponding control cells. We also examined the cell cycle status of CD34⁻KSL and CD34⁺KSL cells on the basis of 5-bromodeoxyuridine (BrdU) incorporation. More BrdU⁺ cells were detected among p57-deficient CD34⁻KSL and CD34⁺KSL populations than among the corresponding control cells (Figure 3C), consistent with the reduced size of the G_0 population for p57-deficient KSL cells. Furthermore, the frequency of apoptosis was substantially increased among p57-deficient KSL cells, but not among p21- or p27-deficient KSL cells (Figure 3D). Similar results were obtained 3 days after the onset of a shortened course of poly(I:C) treatment (Figures S3A–S3D). These results thus suggested that p57, but not p21 or p27, is essential for maintenance of HSC quiescence.

Immunofluorescence analysis revealed that the expression of p53 was increased in p57-deficient KSL cells (Figures S3E and S3F). Treatment of p57-deficient cells with the p53 inhibitor pifithrin- α resulted in suppression of apoptosis and significant restoration of their colony-forming ability (Figures S3G and S3H). Phosphorylation of the retinoblastoma protein (Rb) was increased in p57-deficient KSL cells compared with that in control cells, whereas no such difference was observed between the c-Kit⁺Sca-1⁻Lin⁻ populations of the two genotypes (Figures 3E–3G). Treatment of p57-deficient KSL cells with the chemical CDK inhibitor SU9516, which is relatively specific for CDK2, reversed, at least in part, the changes in colony-forming ability, quiescence, and viability induced by loss of p57 (Figures 3H–3K), suggesting that increased CDK activity contributes to these effects of p57 deletion in KSL cells. Collectively, these results indicated that the loss of p57 results in exhaustion of HSCs, which is attributable in part to the induction of apoptosis mediated by upregulation of CDK activity and p53 expression.

Functional Overlap of p57 with Other CKIs

Although our data indicated that p57 is a key CKI in the determination of stemness of HSCs, it remained possible that other CKIs might partially compensate for the effects of p57 deficiency. To examine this possibility, we generated double-mutant mice that lack both p21 and p57 (Mx1-Cre/p21^{-/-}/p57^{+/-} mice injected with poly(I:C)). Whereas deletion of p57 alone did not affect colony-forming activity of KSL cells in vitro before coculture with OP9 cells (Figure 2F), combined deletion of p21 and p57 resulted in a decrease in such colony formation (Figure 4A). Furthermore, the size of individual colonies was markedly smaller for the double mutant cells than for cells of poly(I:C)-injected Mx1-Cre/p21^{+/+}/p57^{+/+} or Mx1-Cre/p21^{+/+}/p57^{+/-} mice (Figure 4B). The number of colonies formed after coculture with OP9 cells was further decreased for the double-mutant KSL cells compared with that for p57-deficient KSL cells (Figure 4C). However, no significant difference in the percentage of cells in G_0 phase or in the frequency of apoptosis was apparent between KSL cells deficient in p57 alone and those deficient in both p21 and p57 (Figures 4D and 4E). Together, these results suggested that the combined deletion of both CKIs might affect not only HSCs but also progenitor cells. We also examined HSC function in mice lacking both p21 and p27. The number of colonies formed, the percentage of cells in quiescence, and the frequency of apoptosis did not differ significantly between KSL cells derived from p21^{-/-}/p27^{-/-} mice and those derived from wild-type mice (Figures S4A–S4C).

Whereas the members of the Cip/Kip family of CKIs (p21, p27, p57) share a CKI domain that is essential for inhibition of CDKs,

(B and C) Hematopoietic reconstitution capacity of KSL cells (1.5×10^3) (B) or CD150⁺CD48⁻KSL cells (2×10^2) (C) derived from Mx1-Cre/p57^{+/-} or control donor mice at 4 weeks after poly(I:C) injection. BM cells (2×10^6) from the recipient mice in (B) were serially transplanted into additional recipient mice. Data are means \pm SD. ***p < 0.005.

(D) Frequency of donor-derived KSL cells among total BM cells of recipient mice in (B) at 16 weeks after transplantation. Data are means \pm SD. ***p < 0.005.

(E) Irradiated recipient mice were transplanted with donor BM cells (4×10^5) from Mx1-Cre/p57^{+/-} or Mx1-Cre/p57^{+/-} mice (not injected with poly(I:C)) together with an equal number of competitor BM cells. The recipients were injected with poly(I:C) at 4 weeks after transplantation, and the percentage of donor-derived cells in peripheral blood was determined. Data are means \pm SD. ***p < 0.005.

(F) In vitro colony formation capacity of KSL cells from mice of the indicated genotypes with or without prior coculture with OP9 cells. Cells from mice harboring the Mx1-Cre transgene were harvested at 4 weeks after poly(I:C) injection. Data are means \pm SD. ***p < 0.005.

See also Figure S2.

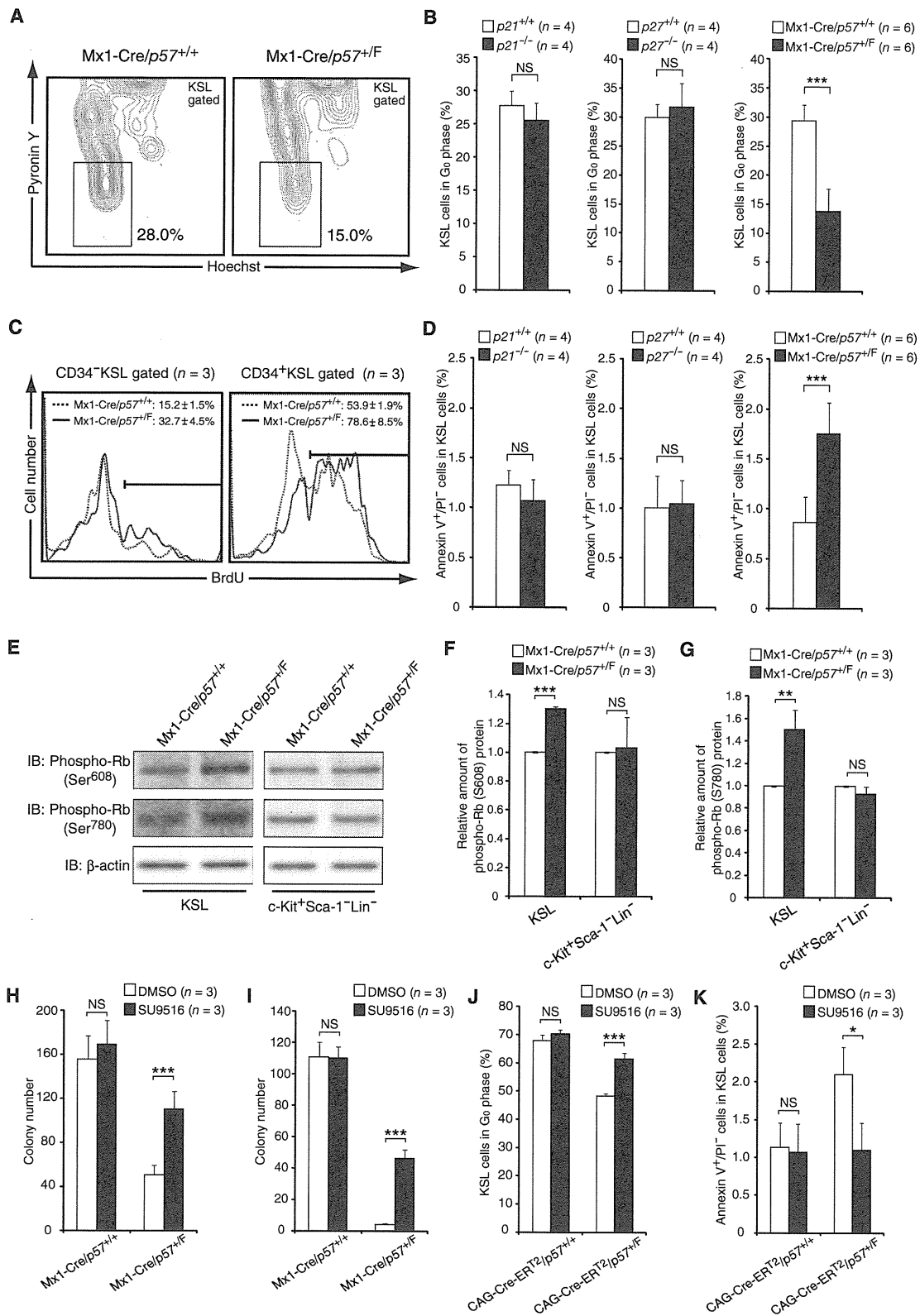


Figure 3. Loss of Quiescence and Induction of Apoptosis due to Increased CDK Activity in p57-Deficient HSCs

(A) Frequency of quiescence in KSL cells of Mx1-Cre/p57^{+/+} and Mx1-Cre/p57^{+F} mice at 4 weeks after poly(I:C) injection. Quiescent cells were detected by staining with Hoechst 33342 and pyronin Y followed by flow cytometry.

p57 also contains a central domain that is absent in p21 and p27 and is thought to mediate functions other than inhibition of CDKs (Matsuoka et al., 1995). To test whether p57 function in the maintenance of HSCs is replaceable by p27, we examined the BM of $p57^{p27KI}$ mice, in which the p57 gene has been replaced with the p27 gene (Susaki et al., 2009). Similar to the pattern of p57 expression in wild-type mice, HA-tagged p27 encoded by the knockin allele at the p57 gene locus was expressed only in the KSL fraction, not in other more differentiated cells (Figure 4F). The size of the KSL population in $p57^{p27KI}$ mice was indistinguishable from that in wild-type mice (Figure 4G), and there was no difference in repopulating capacity at the first BMT, in colony formation in vitro with or without prior coculture with OP9 cells, or in the frequency of quiescence or apoptosis between HSCs of the two genotypes (Figures 4H–4K; Figure S4D). These results suggested that the total abundance of CKIs of the Cip/Kip family is an important determinant of HSC stemness.

DISCUSSION

We have examined the physiological importance of p57 in maintenance of HSCs by analysis of the effects of conditional deletion of p57 in mouse hematopoietic cells. Such mice lacking p57 manifested a reduction in the size of the HSC fraction as well as in the self-renewal capacity and G_0 population of KSL cells, effects that were not observed in mice lacking p21 or p27 (or both). We thus conclude that p57 plays the dominant role among Cip/Kip CKIs in the maintenance of HSCs.

The related CKIs p27 and p57 differ in the spatiotemporal patterns of their expression in many tissues and organs (Nagahama et al., 2001). Whereas p57 is most abundant in the HSC fraction of BM cells, its expression ceases as HSCs differentiate into progenitor cells. Expression of p27 is apparent in all hematopoietic fractions, whereas p21 is not detected in such cells in the absence of genotoxic stress. The expression patterns of these CKIs appear consistent with the phenotypes of the corresponding knockout mice. However, our present results suggest the existence of functional overlap between p57 and its related CKIs. The defects induced by p57 deficiency were thus reversed by p27 knockin, suggesting that the function of these CKIs at the molecular level is indistinguishable. We hypothesize that the specific response of cells to the lack of each CKI might be

dependent on the total CKI abundance rather than on CKI type, but further investigation will be necessary to confirm this hypothesis. This relation between p27 and p57 in HSCs is similar to that observed in most (but not all) other tissues examined (Susaki et al., 2009).

Regulation of the cell cycle is thought to play a key role in the maintenance and function of HSCs. Mutant mice with deletions in genes for various cell cycle regulators thus manifest defects in HSC maintenance and function. The numbers of HSCs as well as common myeloid and lymphoid progenitors are decreased in mice with conditional inactivation of cyclin A2 (Kਾਲaszczynska et al., 2009). The reconstitution ability of BM cells is also markedly impaired in these latter mutant mice. Likewise, mice lacking all D-type cyclins (cyclins D1, D2, and D3) show pronounced BM defects associated with a loss of the reconstitution capacity of BM cells; these animals develop severe anemia and die in utero (Kozar et al., 2004). Similar defects are apparent in mice deficient in both CDK4 and CDK6, which are the major partners of D-type cyclins (Malumbres et al., 2004). In contrast, no abnormality is apparent in mice lacking CDK2 (Berthet et al., 2007), suggesting that CDK1 may compensate for the loss of CDK2 (Aleem et al., 2005).

Rb is a major target of CDK2 and CDK4. $Vav1-Cre/Rb^{F/F}$ mice, which express Cre recombinase in hematopoietic cells, show a marked defect in the self-renewal competence and multipotency of HSCs (Daria et al., 2008), and deletion of all members of the Rb family (Rb, p107, and p130) further exacerbated this phenotype (Viatour et al., 2008). Mice deficient in E2F1, E2F2, and E2F3, all of which are downstream targets of Rb, show a decrease in the number of myeloid cells but maintain the function of HSCs (Viatour et al., 2008).

Some of the members of the Ink4 family of CKIs also contribute to the regulation of HSCs. Expression of $p16^{Ink4a}$ in HSCs increases with age, and the self-renewal capacity of HSCs does not decline with age in mice deficient in this CKI (Janzen et al., 2006). Mice lacking $p15^{Ink4b}$ do not exhibit an apparent defect in HSC function, although the proliferation of progenitors for granulocytes and monocytes is enhanced in these animals (Rosu-Myles et al., 2007). Loss of $p18^{Ink4c}$ results in expansion of the HSC pool associated with promotion of the cell cycle without loss of self-renewal capacity (Yuan et al., 2004). The effects of deletion of Ink4 CKIs thus appear opposite to those of deletion of Cip/Kip CKIs. Deletion of Cip/Kip CKIs results in

(B) Quantitative analysis of quiescent cells among KSL cells from mice of the indicated genotypes as determined from experiments similar to that in (A). Data are means \pm SD. *** p < 0.005.

(C) Frequency of proliferating cells among CD34⁺KSL and CD34⁺KSL cells isolated from $Mx1-Cre/p57^{+/+}$ and $Mx1-Cre/p57^{+/F}$ mice at 4 weeks after poly(I:C) injection. Proliferating cells were detected by BrdU pulse-labeling analysis in vivo. The percentages of BrdU-positive cells are indicated as means \pm SD.

(D) Quantitative analysis of apoptotic cells among KSL cells from mice of the indicated genotypes. Apoptotic cells in the KSL fraction were detected by staining with annexin V and propidium iodide (PI). Data are means \pm SD. *** p < 0.005.

(E) Immunoblot analysis of phosphorylated Rb in KSL and c-Kit⁺Sca-1⁺Lin⁻ cells from $Mx1-Cre/p57^{+/+}$ and $Mx1-Cre/p57^{+/F}$ mice at 4 weeks after poly(I:C) injection.

(F and G) Quantitative analysis of the relative amounts of Ser608-phosphorylated Rb (F) and Ser780-phosphorylated Rb (G) as determined from experiments similar to that in (E). Data are means \pm SD. ** p < 0.01, *** p < 0.005.

(H and I) Colony formation by KSL cells from $Mx1-Cre/p57^{+/+}$ and $Mx1-Cre/p57^{+/F}$ mice at 4 weeks after poly(I:C) injection after coculture on OP9 cells for 2 weeks (H) or 5 weeks (I) with 160 nM SU9516 or dimethyl sulfoxide (DMSO). Data are means \pm SD. *** p < 0.005.

(J and K) Quantitative analysis of quiescent cells (J) and apoptotic cells (K) among KSL cells from $CAG-Cre-ER^{T2}/p57^{+/+}$ and $CAG-Cre-ER^{T2}/p57^{+/F}$ mice after culture for 2 weeks on OP9 cells, the second week in the presence of 1 μ M 4-hydroxytamoxifen (4-OHT) and either 160 nM SU9516 or DMSO. Data are means \pm SD. *** p < 0.005.

See also Figure S3.

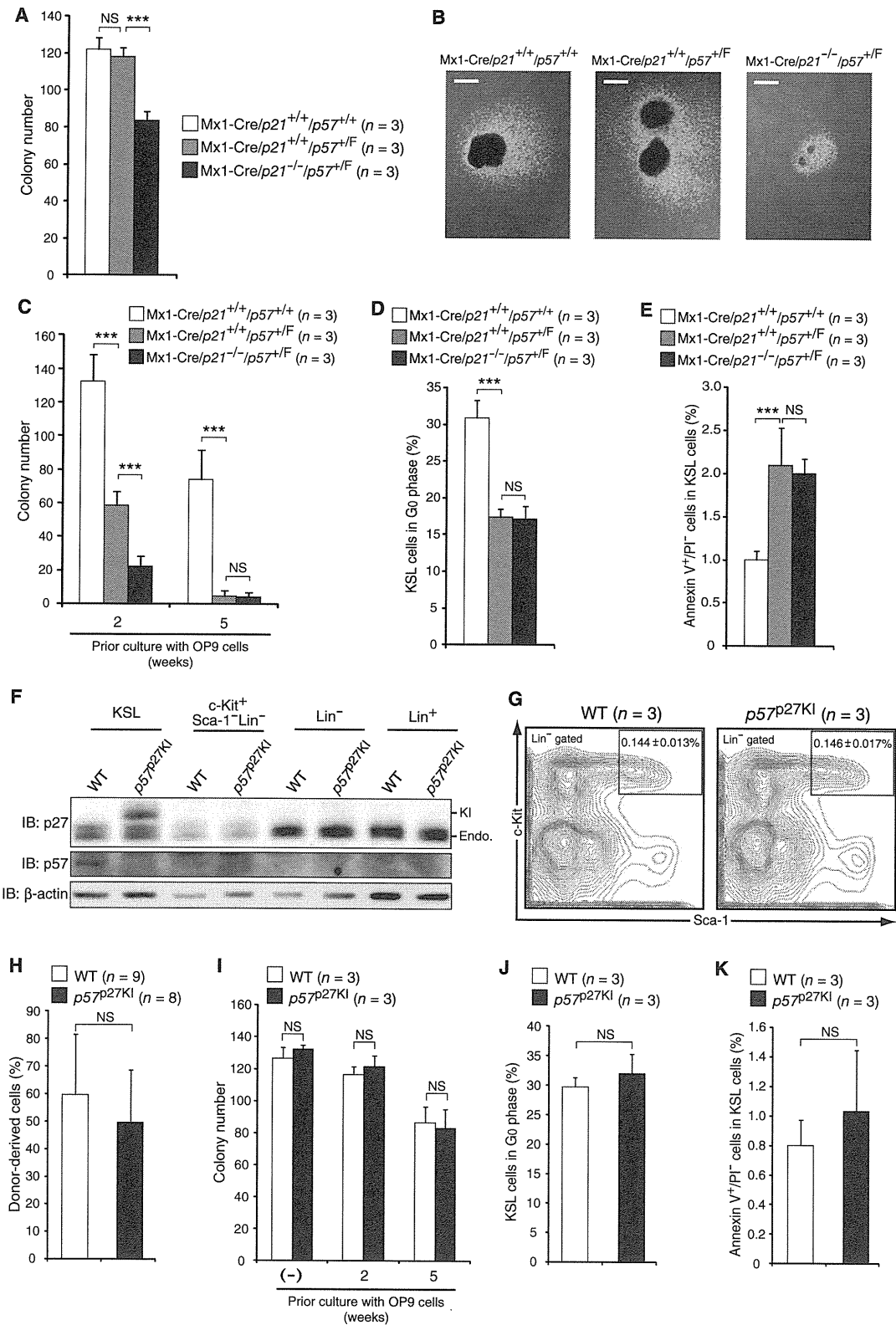


Figure 4. Overlap of CKI Function in HSC Maintenance

(A) In vitro colony formation capacity of KSL cells from mice of the indicated genotypes at 4 weeks after poly(I:C) injection. Data are means ± SD. ***p < 0.005. (B) Representative colonies from the experiment shown in (A). Scale bars represent 0.5 mm.

exit of HSCs from the quiescent state and their entry into the proliferation cycle, an effect that is associated with the loss of self-renewal capacity or promotion of differentiation (or both).

The direct downstream targets of p27 and p57 CKIs are thought to be CDK2 and CDK4 (or CDK6), and inhibition of CDK activity by these CKIs maintains Rb in the unphosphorylated state (Halaban, 2005). Our results now show that the phosphorylation of Rb on Ser608 (phosphorylated by CDK2-cyclin A or E and CDK4-cyclin D) and Ser780 (phosphorylated by CDK4-cyclin D) (Halaban, 2005) was increased in p57-deficient KSL cells, suggesting that the activity of CDK2 or CDK4 (or both) is increased in KSL cells by deletion of p57.

We examined whether the effects of p57 deletion in HSCs are reversed by inhibition of CDK activity with the use of the chemical CDK inhibitor SU9516, which is relatively specific for CDK2 (Moshinsky et al., 2003). The in vitro colony formation capacity of KSL cells from poly(I:C)-injected Mx1-Cre/p57^{+/-} mice was partially restored by treatment with SU9516 during prior coculture with OP9 cells, suggesting that increased activity of CDK2 is probably responsible for the effects of p57 deletion in KSL cells. The partial, rather than complete, restoration might be attributable to a contribution of CDK4 to the downregulation of colony formation ability in the p57-deficient KSL cells.

We have also shown that treatment of p57-deficient KSL cells with the p53 inhibitor pifithrin- α suppressed apoptosis and partially restored colony-forming ability. Furthermore, we have independently demonstrated that ablation of p57 results in hyperactivation of E2F1 and consequent p53-mediated apoptosis in mice (Susaki et al., 2009). Together, these lines of evidence support the notion that p57 deficiency results in abnormal upregulation of CDK activity, leading to hyperactivation of E2F1 and the triggering of p53-dependent apoptosis.

One of the substantial differences between fetal and adult HSCs is their dependency on quiescence: Maintenance of quiescence is thus thought to be more important for adult HSCs than for fetal HSCs. In an accompanying paper (Zou et al., 2011 [this issue of *Cell Stem Cell*]), HSCs in the fetal liver of conventional p27- or p57-deficient mice (Nakayama et al., 1996; Takahashi et al., 2000) were analyzed. Fetal HSCs lacking p57 did not manifest an apparent defect with the exception of a slight decrease in BM reconstitution capacity that was observed only after the third round of BM transfer. Combined deletion of p27 and p57 resulted in a marked failure in the maintenance of fetal HSCs, however, suggesting that these two CKIs have redundant roles. In contrast, our present study shows that p57 deficiency alone results in a substantial decrease in the number of adult HSCs as a result of their exit from quiescence and entry into apoptosis, with the BM reconstitution capacity of these

p57-deficient cells also being greatly reduced from the first round of BM transfer. Deletion of p21 or p27 (or both proteins) did not result in any overt abnormalities in adult HSCs. Our analysis of mice lacking both p21 and p57 suggests that p21 also contributes to the maintenance of hematopoiesis, and that of p57^{p27^{KI}} mice suggests that p57 function in HSC maintenance can be replaced by p27. Collectively, our present study demonstrates that p57 plays a predominant role in constitutive maintenance of HSCs after birth.

EXPERIMENTAL PROCEDURES

Mice

Detailed methods for the generation of mice heterozygous for the floxed p57 allele (p57^{+/-} mice) as well as other mice used in this study are described in Supplemental Experimental Procedures. All mice were backcrossed with C57BL/6 mice more than six times. All mouse experiments were approved by the animal ethics committee of Kyushu University.

BM Reconstitution Assays

Unfractionated BM cells (4×10^5), sorted LSK cells (1.5×10^3), or sorted CD150⁺CD48⁻LSK cells (2×10^2) from p21^{-/-}, p27^{-/-}, Mx1-Cre/p57^{+/-}, or corresponding littermate control mice (CD45.2) were transplanted into lethally irradiated C57BL/6 congenic (CD45.1) recipients together with competitor BM cells (4×10^5) from C57BL/6 heterozygous congenic (CD45.1/CD45.2) mice. For serial transplantation analysis, BM cells (2×10^6) were obtained from recipient mice at 16 weeks after transplantation (first BMT) and were transferred to a second set of lethally irradiated mice (second BMT).

Colony Formation Assays

Sorted KSL cells were subjected to colony formation assays with or without prior coculture with OP9 cells. Detailed methods for the assays are described in Supplemental Experimental Procedures.

SUPPLEMENTAL INFORMATION

Supplemental Information includes Supplemental Experimental Procedures and four figures and can be found with this article online at doi:10.1016/j.stem.2011.06.014.

ACKNOWLEDGMENTS

We thank P. Leder for p21-deficient mice, Y. Fukui for Ella-Cre transgenic mice, D.R. Littman for pL2-Neo and pMC-Cre, T. Suda for sharing unpublished results, and Y. Matsuzaki, K. Shibata, A. Niihara, C. Mitai, Y. Yamada, K. Takeda, and M. Tanaka for technical assistance.

Received: December 13, 2010

Revised: June 1, 2011

Accepted: June 27, 2011

Published: September 1, 2011

(C) In vitro colony formation capacity of KSL cells from mice of the indicated genotypes after coculture with OP9 cells. Data are means \pm SD. ***p < 0.005.

(D and E) Quantitative analysis of quiescent cells (D) and apoptotic cells (E) among KSL cells from mice of the indicated genotypes. Data are means \pm SD. ***p < 0.005.

(F) Immunoblot analysis of fractionated hematopoietic cells from BM of wild-type (WT) and p57^{p27^{KI}} mice. The band positions for endogenous p27 (Endo.) and knocked-in hemagglutinin epitope-tagged p27 (KI) are shown.

(G) Frequency of KSL cells among BM cells of wild-type and p57^{p27^{KI}} mice. The percentages of KSL cells among total BM cells are shown as means \pm SD.

(H) Hematopoietic reconstitution capacity of BM cells from p57^{p27^{KI}} and littermate control mice. Data are means \pm SD.

(I) In vitro colony formation capacity of KSL cells from wild-type and p57^{p27^{KI}} mice with or without prior coculture with OP9 cells. Data are means \pm SD.

(J and K) Quantitative analysis of quiescent cells (J) and apoptotic cells (K) among KSL cells from wild-type and p57^{p27^{KI}} mice. Data are means \pm SD.

See also Figure S4.

REFERENCES

- Aleem, E., Kiyokawa, H., and Kaldis, P. (2005). Cdc2-cyclin E complexes regulate the G1/S phase transition. *Nat. Cell Biol.* 7, 831–836.
- Arai, F., and Suda, T. (2007). Maintenance of quiescent hematopoietic stem cells in the osteoblastic niche. *Ann. N Y Acad. Sci.* 1106, 41–53.
- Berthet, C., Rodriguez-Galan, M.C., Hodge, D.L., Gooya, J., Pascal, V., Young, H.A., Keller, J., Bosselut, R., and Kaldis, P. (2007). Hematopoiesis and thymic apoptosis are not affected by the loss of Cdk2. *Mol. Cell. Biol.* 27, 5079–5089.
- Cheng, T., Rodrigues, N., Dombkowski, D., Stier, S., and Scadden, D.T. (2000a). Stem cell repopulation efficiency but not pool size is governed by p21^{Cip1}. *Nat. Med.* 6, 1235–1240.
- Cheng, T., Rodrigues, N., Shen, H., Yang, Y., Dombkowski, D., Sykes, M., and Scadden, D.T. (2000b). Hematopoietic stem cell quiescence maintained by p21^{Cip1/Waf1}. *Science* 287, 1804–1808.
- Daria, D., Filippi, M.D., Knudsen, E.S., Faccio, R., Li, Z., Kalfa, T., and Geiger, H. (2008). The retinoblastoma tumor suppressor is a critical intrinsic regulator for hematopoietic stem and progenitor cells under stress. *Blood* 111, 1894–1902.
- Halaban, R. (2005). Rb/E2F: A two-edged sword in the melanocytic system. *Cancer Metastasis Rev.* 24, 339–356.
- Janzen, V., Forkert, R., Fleming, H.E., Saito, Y., Waring, M.T., Dombkowski, D.M., Cheng, T., DePinho, R.A., Sharpless, N.E., and Scadden, D.T. (2006). Stem-cell ageing modified by the cyclin-dependent kinase inhibitor p16^{Ink4a}. *Nature* 443, 421–426.
- Kalaszczynska, I., Geng, Y., Iino, T., Mizuno, S., Choi, Y., Kondratiuk, I., Silver, D.P., Wolgemuth, D.J., Akashi, K., and Sicinski, P. (2009). Cyclin A is redundant in fibroblasts but essential in hematopoietic and embryonic stem cells. *Cell* 138, 352–365.
- Kozar, K., Ciemerych, M.A., Rebel, V.I., Shigematsu, H., Zagodzón, A., Sicinska, E., Geng, Y., Yu, Q., Bhattacharya, S., Bronson, R.T., et al. (2004). Mouse development and cell proliferation in the absence of D-cyclins. *Cell* 118, 477–491.
- Lakso, M., Pichel, J.G., Gorman, J.R., Sauer, B., Okamoto, Y., Lee, E., Alt, F.W., and Westphal, H. (1996). Efficient *in vivo* manipulation of mouse genomic sequences at the zygote stage. *Proc. Natl. Acad. Sci. USA* 93, 5860–5865.
- Malumbres, M., Sotillo, R., Santamaría, D., Galán, J., Cerezo, A., Ortega, S., Dubus, P., and Barbacid, M. (2004). Mammalian cells cycle without the D-type cyclin-dependent kinases Cdk4 and Cdk6. *Cell* 118, 493–504.
- Matsuoka, S., Edwards, M.C., Bai, C., Parker, S., Zhang, P., Baldini, A., Harper, J.W., and Elledge, S.J. (1995). p57^{KIP2}, a structurally distinct member of the p21^{CIP1} Cdk inhibitor family, is a candidate tumor suppressor gene. *Genes Dev.* 9, 650–662.
- Miyamoto, K., Araki, K.Y., Naka, K., Arai, F., Takubo, K., Yamazaki, S., Matsuoka, S., Miyamoto, T., Ito, K., Ohmura, M., et al. (2007). Foxo3a is essential for maintenance of the hematopoietic stem cell pool. *Cell Stem Cell* 1, 101–112.
- Moshinsky, D.J., Bellamacina, C.R., Boisvert, D.C., Huang, P., Hui, T., Jancarik, J., Kim, S.H., and Rice, A.G. (2003). SU9516: Biochemical analysis of cdk inhibition and crystal structure in complex with cdk2. *Biochem. Biophys. Res. Commun.* 310, 1026–1031.
- Nagahama, H., Hatakeyama, S., Nakayama, K., Nagata, M., Tomita, K., and Nakayama, K. (2001). Spatial and temporal expression patterns of the cyclin-dependent kinase (CDK) inhibitors p27^{KIP1} and p57^{KIP2} during mouse development. *Anat. Embryol. (Berl.)* 203, 77–87.
- Nakayama, K., Ishida, N., Shirane, M., Inomata, A., Inoue, T., Shishido, N., Horii, I., Loh, D.Y., and Nakayama, K.I. (1996). Mice lacking p27^{KIP1} display increased body size, multiple organ hyperplasia, retinal dysplasia, and pituitary tumors. *Cell* 85, 707–720.
- Pawliuk, R., Eaves, C., and Humphries, R.K. (1996). Evidence of both ontogeny and transplant dose-regulated expansion of hematopoietic stem cells *in vivo*. *Blood* 88, 2852–2858.
- Qian, H., Buza-Vidas, N., Hyland, C.D., Jensen, C.T., Antonchuk, J., Månsson, R., Thoren, L.A., Ekblom, M., Alexander, W.S., and Jacobsen, S.E.W. (2007). Critical role of thrombopoietin in maintaining adult quiescent hematopoietic stem cells. *Cell Stem Cell* 1, 671–684.
- Rosu-Myles, M., Taylor, B.J., and Wolff, L. (2007). Loss of the tumor suppressor p15^{Ink4b} enhances myeloid progenitor formation from common myeloid progenitors. *Exp. Hematol.* 35, 394–406.
- Sherr, C.J., and Roberts, J.M. (2004). Living with or without cyclins and cyclin-dependent kinases. *Genes Dev.* 18, 2699–2711.
- Susaki, E., Nakayama, K., Yamasaki, L., and Nakayama, K.I. (2009). Common and specific roles of the related CDK inhibitors p27 and p57 revealed by a knock-in mouse model. *Proc. Natl. Acad. Sci. USA* 106, 5192–5197.
- Takahashi, K., Nakayama, K., and Nakayama, K.I. (2000). Mice lacking a CDK inhibitor, p57^{KIP2}, exhibit skeletal abnormalities and growth retardation. *J. Biochem.* 127, 73–83.
- van Os, R., Kamminga, L.M., Ausema, A., Bystrykh, L.V., Draijer, D.P., van Pelt, K., Dontje, B., and de Haan, G. (2007). A limited role for p21^{Cip1/Waf1} in maintaining normal hematopoietic stem cell functioning. *Stem Cells* 25, 836–843.
- Viatour, P., Somervaille, T.C., Venkatasubrahmanyam, S., Kogan, S., McLaughlin, M.E., Weissman, I.L., Butte, A.J., Passegué, E., and Sage, J. (2008). Hematopoietic stem cell quiescence is maintained by compound contributions of the retinoblastoma gene family. *Cell Stem Cell* 3, 416–428.
- Yamazaki, S., Iwama, A., Takayanagi, S.I., Morita, Y., Eto, K., Ema, H., and Nakauchi, H. (2006). Cytokine signals modulated via lipid rafts mimic niche signals and induce hibernation in hematopoietic stem cells. *EMBO J.* 25, 3515–3523.
- Yan, Y., Frisén, J., Lee, M.H., Massagué, J., and Barbacid, M. (1997). Ablation of the CDK inhibitor p57^{KIP2} results in increased apoptosis and delayed differentiation during mouse development. *Genes Dev.* 11, 973–983.
- Yuan, Y.Z., Shen, H.M., Franklin, D.S., Scadden, D.T., and Cheng, T. (2004). *In vivo* self-renewing divisions of haematopoietic stem cells are increased in the absence of the early G1-phase inhibitor, p18^{Ink4C}. *Nat. Cell Biol.* 6, 436–442.
- Zhang, P., Liégeois, N.J., Wong, C., Finegold, M., Hou, H., Thompson, J.C., Silverman, A., Harper, J.W., DePinho, R.A., and Elledge, S.J. (1997). Altered cell differentiation and proliferation in mice lacking p57^{KIP2} indicates a role in Beckwith-Wiedemann syndrome. *Nature* 387, 151–158.
- Zou, P., Arai, F., Yoshihara, H., Tai, I., Hosokawa, K., Matsumoto, Y., Shimmyozu, K., Tsukahara, F., Maru, Y., Nakayama, K., et al. (2011). p57^{KIP2} and p57^{KIP1} cooperate to maintain hematopoietic stem cell quiescence through interactions with Hsc70. *Cell Stem Cell* 9, this issue, 247–261.